ELSEVIER

Institut Pasteur

Microbes and Infection 16 (2014) 936–944

www.elsevier.com/locate/micinf

Original article

Distinct combinations of amino acid substitutions in *N*-terminal domain of Gag-capsid afford HIV-1 resistance to rhesus TRIM5α

Masako Nomaguchi [a], Emi E. Nakayama [b], Masaru Yokoyama [c], Naoya Doi [a,d], Tatsuhiko Igarashi [e], Tatsuo Shioda [b], Hironori Sato [c], Akio Adachi [a,*]

[a] *Department of Microbiology, Institute of Health Biosciences, The University of Tokushima Graduate School, Tokushima, Tokushima, Japan*
[b] *Department of Viral Infections, Research Institute for Microbial Diseases, Osaka University, Suita, Osaka, Japan*
[c] *Laboratory of Viral Genomics, Pathogen Genomics Center, National Institute of Infectious Diseases, Musashimurayama, Tokyo, Japan*
[d] *Japanese Foundation for AIDS Prevention, Chiyoda-ku, Tokyo, Japan*
[e] *Laboratory of Primate Model, Experimental Research Center for Infectious Diseases, Institute for Virus Research, Kyoto University, Kyoto, Kyoto, Japan*

Received 18 June 2014; accepted 27 August 2014
Available online 4 September 2014

Abstract

TRIM5α is a potent anti-retroviral factor that interacts with viral capsid (CA) in a species-specific manner. Recently, we and others reported generation of two distinct HIV-1 CAs that effectively overcome rhesus TRIM5α-imposed species barrier. In this study, to directly compare the effect of different mutations in the two HIV-1 CAs on evasion from macaque TRIM5-restriction, we newly generated macaque-tropic HIV-1 (HIV-1mt) proviral clones carrying the distinct CAs in the same genomic backbone, and examined their replication abilities in macaque TRIM5-overexpressing human cells and in rhesus cells. Comparative analysis of amino acid sequences and homology modeling-based structures revealed that, while both CAs gained some mutated amino acids with similar physicochemical properties, their overall appearances of N-terminal domains were different. Experimentally, the two CAs exhibited incomplete TRIM5α-resistance relative to SIVmac239 CA and different degrees of susceptibility to various TRIM5 proteins. Finally, two HIV-1mt clones carrying a different combination of the CA mutations were found to grow to a comparable extent in established and primary rhesus cells. Our data show that there could be some distinct CA patterns to confer significant TRIM5-resistance on HIV-1.

Keywords: HIV-1; HIV-1mt; Capsid; Gag-CA; Rhesus macaque; TRIM5α

1. Introduction

TRIM5α interacts with retroviral Gag-capsid (CA) and inhibits viral replication in a species-specific manner [1–6]. TRIM5α acts as a pattern-recognition molecule via its C-terminal B30.2/SPRY domain on diverse retroviral CAs [7–12]. It is proposed that retroviruses overcome TRIM5α-restriction either by mutating CA to abolish recognition by TRIM5α B30.2/SPRY domain, or by altering a surface pattern of CA lattice [9]. Macaque TRIM5α is one of the major species-barriers for HIV-1. Evasion from macaque TRIM5α-restriction would facilitate establishing HIV-1/macaque models useful for basic and clinical AIDS studies [13,14]. Recently, we successfully generated rhesus macaque (RhM) TRIM5α-resistant HIV-1 CA, designated LSDQ (Fig. 1A), through comparative sequence/structure analyses of HIV and SIVmac239 CAs [15]. Soll et al. also constructed RhM TRIM5α-resistant HIV-1 CA, designated LNEIE (Fig. 1A), by "assisted evolution" method [16]. Interestingly, LSDQ and LNEIE CAs have different amino acid substitutions that contribute to TRIM5α-resistance. Furthermore, a virus carrying LSDQ CA or LNEIE CA grew best in RhM peripheral blood

* Corresponding author. Tel.: +81 88 633 7078; fax: +81 88 633 7080.
E-mail address: adachi@basic.med.tokushima-u.ac.jp (A. Adachi).

http://dx.doi.org/10.1016/j.micinf.2014.08.017
1286-4579/

A

```
                β-hairpin          Helix1              Helix2        Helix3      Helix4
NL4-3   1 PIVQNLQGQMVHQAISPRTLNAWVKVVEEKAFSPEVIPMFSALSEGATPQDLNTMLNTVGGHQAAMQMLK 70
LNEIE   1 .........L.............................................................. 70
LSDQ    1 .............................................................................. 70
MA239   1 .-..QIG.NY..LPL.........LI...K.GA..V.G.Q.....C..Y.I.Q...C..D......IIR 69

                                CypA
                Helix4          binding loop    Helix5      Helix6          Helix7
NL4-3  71 ETINEEAAEWDRLHPVHAGPIAPGQMREPRGSDIAGTTSTLQEQIGWMTHNP-PIPVGEIYKRWIILGLN 139
LNEIE  71 ...................NE...I...................E.......-.................. 139
LSDQ   71 ...............QP.-.QQ-..L...S...........D...Q...RQQN.................. 138
MA239  70 DI......D..LQ..QP.-.QQ-..L...S.........SVD...Q..YRQQN.....N..R...Q...Q 137
```

B

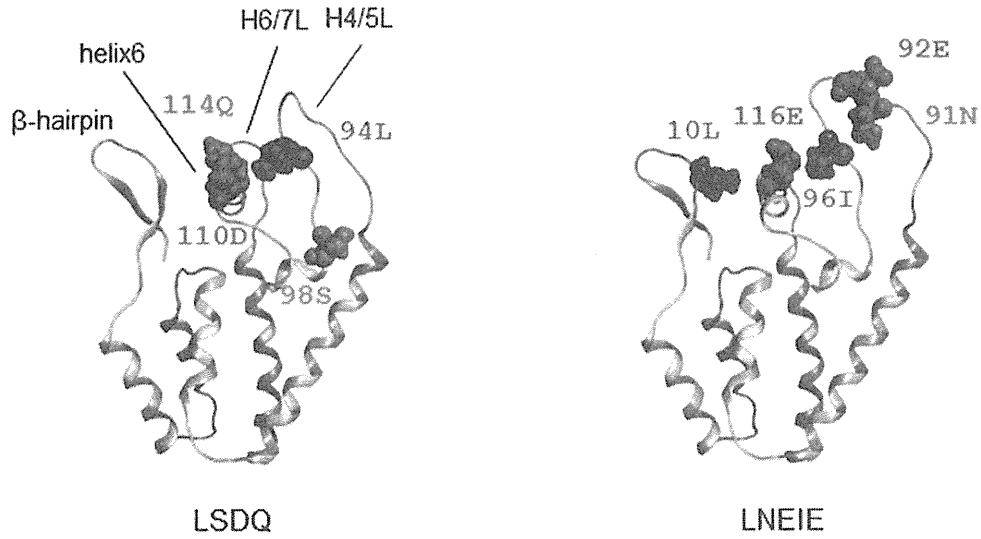

C

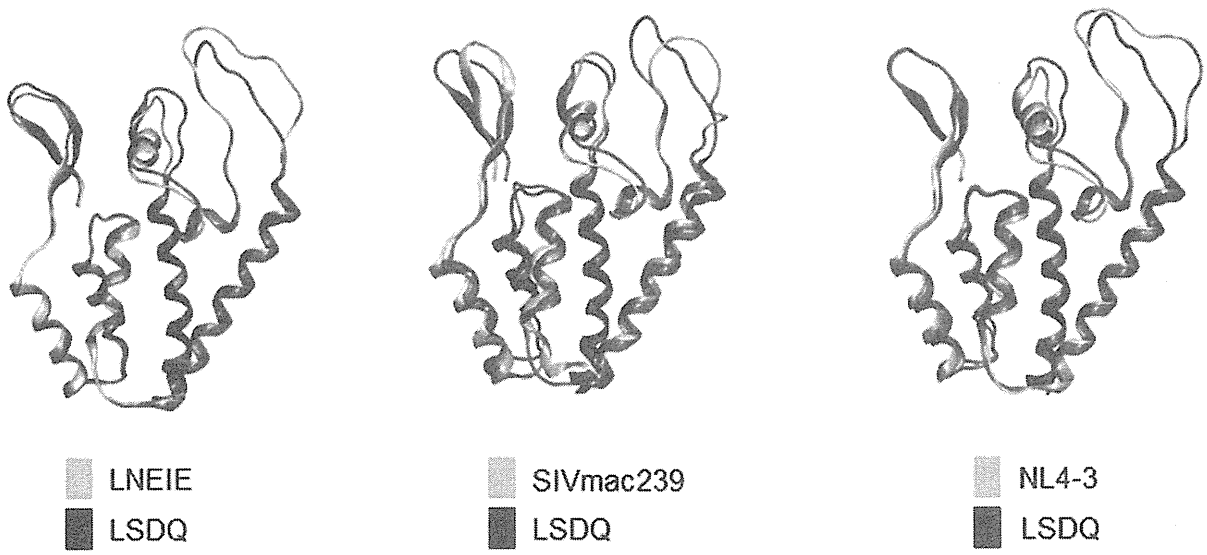

Fig. 1. Structure of CA NTD from two different HIV-1mt clones. (A) Alignment of CA sequences. Amino acid sequences in CA (amino acid residues 1 to 137/138/139) of HIV-1_{NL4-3} (GenBank: AF324493), LNEIE [16], LSDQ [15], and SIVmac239 (GenBank: M33262) were aligned by Genetix ver. 11. Dots show the same amino acid residues with those of HIV-1_{NL4-3}. Hyphens indicate the gap. The domains of β-hairpin and helices 1 to 7 are indicated based on the previous publication [37]. (B) Structural models for CA NTD from two distinct HIV-1mt clones LSDQ and LNEIE. Molecular models were constructed by homology modeling and were refined as previously described [15]. HIV-1 CA NTD at a resolution of 1.95Å (PDB code: 4LQW) [20] was used as modeling template. (C) Superimposition of the CA structures. Superposed structures of LNEIE/LSDQ CAs (left), SIVmac239 (modified structure of PDB code 4HTW)/LSDQ CAs (middle), and NL4-3 (PDB code 3GV2)/LSDQ CAs (right) are shown using two different colors indicated.

mononuclear cells (PBMCs) among the macaque-tropic HIV-1 (HIV-1mt) clones examined in each study [15,16]. In this work, we aimed to gain virological and structural insights into evasion from TRIM5α-restriction using the two distinct HIV-1 CAs.

2. Materials and methods

2.1. Plasmid DNA

An HIV-1mt clone designated MN4/LSDQgtu and a standard SIVmac clone designated SIVmac239 used in this study were described previously [15]. Clone pLNEIE was constructed by introduction of the five mutations [16] into the CA-coding region of a sub-genomic clone derived from pNL4-3 by QuickChange Site-Directed Mutagenesis kit (Agilent Technologies Inc., Santa Clara, CA). Clone pSCA was constructed from the above sub-genomic clone by overlapping PCR and QuickChange Site-Directed Mutagenesis kit to have Gag sequences as described for stHIV-1_{SCA} [16,17]. Proviral clones designated LSDQ+4gtu, LNEIE+4gtu, and SCA+4gtu were generated by replacement of the *Bss*HII-*Sbf*I DNA fragment of MN4/LSDQgtu with the corresponding fragments of "MN4/LSDQgtu", pLNEIE, and pSCA clones, respectively.

2.2. Cell culture, virus preparation, and reverse transcriptase (RT) assays

A human kidney cell line 293T, a RhM lymphocytic cell line M1.3S and RhM PBMCs were cultured as described previously [15]. The *TRIM5* genotypes of PBMCs, prepared from RhM individuals and used for infection experiments, were determined as described previously [15]. Virus stocks were prepared from 293T cells transfected with proviral clones on day 2 post-transfection. Virus stocks were assayed for RT activities, and used for infection experiments as previously described [15].

2.3. TRIM5 susceptibility assays

TRIM5 susceptibility assays in human MT4 cells were done by the recombinant Sendai virus (SeV)-TRIM5 expression system as described previously [15,18].

2.4. Multi-cycle virus replication assays

Infection of M1.3S cells was ordinarily performed as described previously [15]. For infection of RhM PBMCs, the spinoculation method [19] was used. Virus replication was monitored by RT activity released into the culture supernatants.

2.5. Structural analysis

Molecular models for HIV-1mt CA N-terminal domain (NTD) were constructed by homology modeling and were refined as described previously [15]. HIV-1 CA NTD at a resolution of 1.95Å (PDB code: 4LQW) [20] was used as modeling template. Superimpositions of the structures were done using the Protein Superpose module in MOE (Chemical Computing Group Inc., Quebec, Canada).

3. Results

3.1. Sequence and structure comparison of LSDQ and LNEIE CAs

Determinants in retroviral CA to modulate TRIM5α-susceptibility have been mapped to CA surface domains including β-hairpin, a loop between helices 4 and 5 (H4/5L), helix6, and H6/7L (Fig. 1A) [15,18,21–29]. LSDQ and LNEIE, the two RhM TRIM5α-resistant HIV-1 CAs, have different amino acid sequences, convergently in a cyclophillin A (CypA) binding loop within H4/5L and in H6/7L. The loop regions in LSDQ CA have been replaced with those in SIVmac239 CA (Fig. 1A). As indicated in Fig. 1B, LSDQ and LNEIE CAs commonly gained a negatively charged amino acid residue in helix6 (110D for LSDQ and 116E for LNEIE) and paired substitutions in helix6 and H4/5L (114Q/94L for LSDQ and 116E/96I for LNEIE). However, the overall appearance of CA NTD was different between the two clones mainly due to difference in H4/5L- and H6/7L-length, which could affect a surface pattern of viral core (Fig. 1C, left). In addition, the structure of LSDQ CA was different from those of its parental CAs, i.e., SIVmac239 and NL4-3 CAs, especially in the H4/5L region (Fig. 1C, middle and right). Moreover, the β-hairpin domain of SIVmac239 CA was structurally distinct from those of LSDQ, LNEIE, and NL4-3 CAs (Fig. 1C). Conclusively, LSDQ and LNEIE CAs are structurally unique to each other (Fig. 1), but both contribute to the TRIM5α-resistance [15,16].

3.2. LSDQ and LNEIE CAs exhibit different susceptibilities to the restriction mediated by various macaque TRIM5 proteins

To examine potentials of the two distinct CAs for evading TRIM5α-restriction and for viral replication, we constructed new proviral clones in the backbone of our best HIV-1mt designated MN4/LSDQgtu (Fig. 2A) [15]. The *Bss*HII-*Sbf*I DNA fragment of MN4/LSDQgtu was replaced with the corresponding fragments of LNEIE [16] and LSDQ [15] to generate LNEIE+4gtu and LSDQ+4gtu, respectively. The sequence differences between the two clones reside only in the CA NTD (Fig. 1A).

First, we determined susceptibility of LSDQ+4gtu and LNEIE+4gtu to various TRIM5 proteins expressed by SeV vectors. Ability of viral clones to evade TRIM5-restriction, in comparison with that of SIVmac239, can be readily determined by this recombinant SeV-TRIM5 overexpression system [15,18]. Macaque TRIM5 alleles are divided into three functionally different groups: $TRIM5\alpha^{TFP}$, $TRIM5\alpha^{Q}$, and $TRIM5^{CypA}$ [30–32]. TRIM5α proteins of both RhM and cynomolgus macaque (CyM), and CyM TRIM5CypA inhibit HIV-1 replication, but not RhM TRIM5CypA [33,34]. Thus,

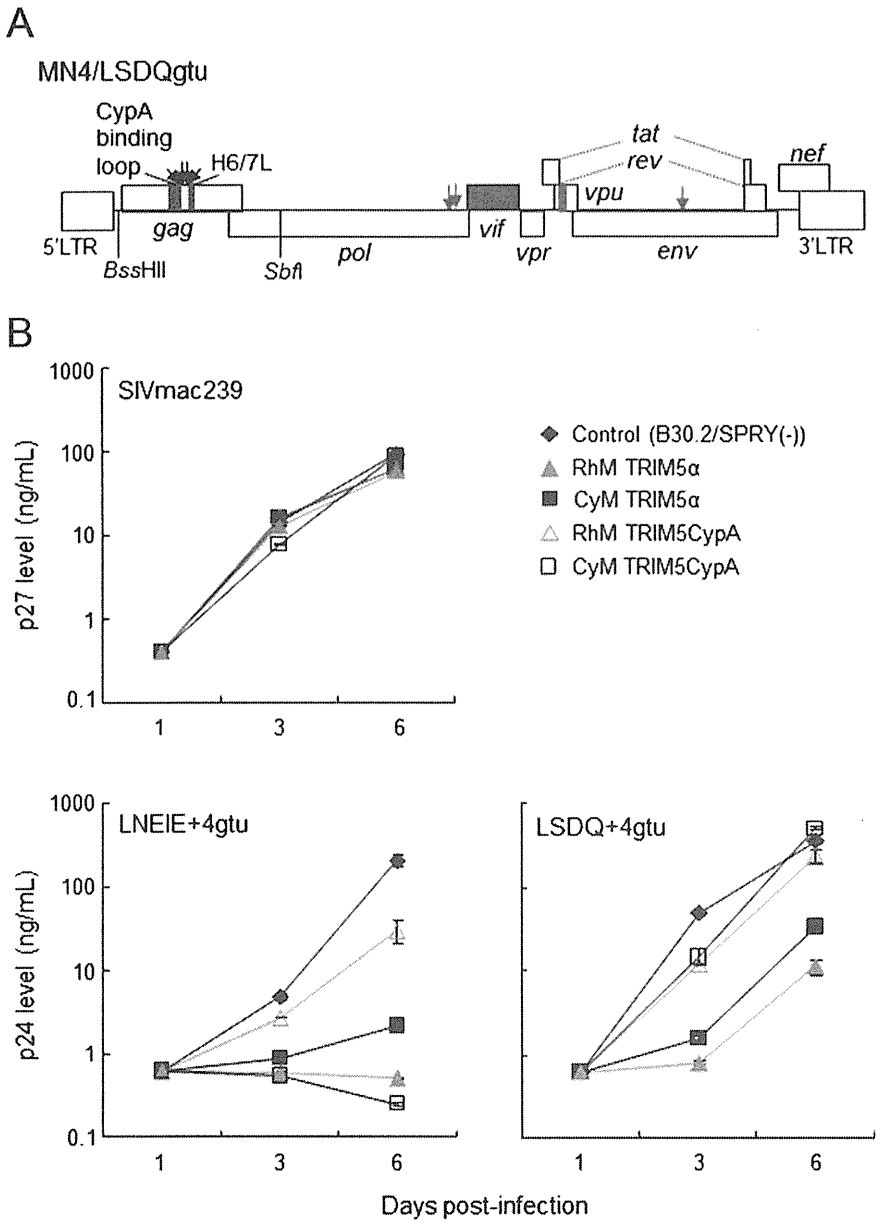

Fig. 2. Susceptibility of viral clones to various macaque TRIM5 proteins. (A) Proviral genome structure of an HIV-1mt clone MN4/LSDQgtu [15]. Blue and red areas show sequences from SIVmac239 and SIVgsn166 (SIV isolated from the greater spot-nosed monkey) (GenBank: AF468659), respectively. Green arrows show the adaptive mutations that enhance the viral growth potential [38]. Four amino acid substitutions (M94L/R98S/Q110D/G114Q) in CA that increase RhM TRIM5α-resistance are indicated by black arrows [15]. The *Bss*HII and *Sbf*I sites used for construction of MN4/LSDQgtu-based viral clones carrying distinct CAs are indicated. (B) TRIM5 susceptibility assays. Human MT4 cells (1.0×10^5) were infected with recombinant SeV expressing B30.2/SPRY (−) TRIM5, CyM TRIM5α (*TRIM5α*^{Q}), RhM TRIM5α (*TRIM5α*^{TFP}), CyM TRIM5CypA (*TRIM5*^{CypA}), or RhM TRIM5CypA (*TRIM5*^{CypA}). B30.2/SPRY (−) TRIM5 without the ability to restrict viral replication served as a control. Nine hours after infection with recombinant SeVs, cells were super-infected with 20 ng (Gag-p24) of HIV-1mt clones or 20 ng (Gag-p27) of SIVmac239. Virus replication was monitored by the amount of Gag-p24 (HIV-1mt clones) or Gag-p27 (SIVmac239) in the culture supernatants. Error bars show fluctuations between duplicate samples. Representative data from two independent experiments are shown. (For interpretation of the references to color in this figure legend, the reader is referred to the web version of this article.)

we tested here four different TRIM5 alleles, i.e., RhM TRIM5α (*TRIM5α*^{TFP}), CyM TRIM5α (*TRIM5α*^{Q}), RhM TRIM5CypA (*TRIM5*^{CypA}), and CyM TRIM5CypA (*TRIM5*^{CypA}), using B30.2/SPRY(−) TRIM5 as a control. As shown in Fig. 2B, SIVmac239 replicated similarly well in the presence of RhM TRIM5α, CyM TRIM5α, RhM TRIM5-CypA, or CyM TRIM5CypA as in control cells expressing B30.2/SPRY(−) TRIM5. While not complete as compared with the case of SIVmac239 [15], LSDQ+4gtu showed more resistance to various RhM/CyM TRIM5 proteins than LNEIE+4gtu. In particular, consistent with previous observations, LSDQ+4gtu replicated well in the presence of CyM TRIMCypA, but not at all LNEIE+4gtu [15,16]. Furthermore, in the presence CyM/RhM TRIM5α, LNEIE+4gtu appeared to replicate (note the data in the presence of CyM TRIM5-CypA in Fig. 2B) but clearly more poorly than LSDQ+4gtu.

Table 1
Lethal mutations in CA of MN4/LSDQgtu.[a]

Mutants	CA mutations relative to LSDQ	CA domains	References
P37S-LSDQ	P38S	Helix2	[35]
LSVDQ	L109V	Helix6	[25]
LSDQY	T117Y	Helix6	
LSVDQY	L109V/T117Y	Helix6	
Mutants of β-hairpin domain	Amino acid sequences in β-hairpin[b]		
LSDQ (parental clone)	PIVQNLQGQMVHQAI		[15]
Wild-type SIVmac239	PVQQIGGNYVHLPL		
M10L-LSDQ	PIVQNLQGQ**L**VHQAI		[16]
Q13L-LSDQ	PIVQNLQGQMVH**L**AI		
IGGN-LSDQ	PIVQ**IGGN**MVHQAI		
Beta-1	P**VQ**Q**IGGN**MVHQAI		
Beta-2	PIVQ**IGGNY**VH**L**AI		
Beta-3	PIVQNLQGQMVH**LPL**		
Beta-4	P**VQ**QNLQGQMVHQAI		
Beta-5	PIVQ**IGGNY**VHQAI		
Beta-6	P**VQ**Q**IGGNY**VH**L**AI		
Beta-7	P**VQ**Q**IGGNY**VH**LPL**		
Beta-8	PIVQ**IGGNY**VH**LPL**		

[a] Lethal mutations as judged by viral replication in M1.3S cells during the observation period (15 days).
[b] Bold letters show the mutations introduced into LSDQ CA. For alignment of four CA NTD sequences, see Fig. 1A.

These results show that LSDQ and LNEIE have intrinsically different abilities to negotiate anti-viral effects of various macaque TRIM5 proteins.

Amino acid substitutions in CA contributing to escape from RhM TRIM5α-restriction have been identified by *in vivo* adaptation of SIVsm (SIV from the sooty mangabey) in RhM (P37S and R97S in SIVsm CA) [30,35], and by "gain-of-sensitivity assays" using SIVmac239 CA (L93M, S97R, V108L, D109Q, and Q113G) [25]. TRIM5-resistant LSDQ CA already has M94L, R98S, Q110D, and G114Q mutations corresponding to L93, S97, D109, and Q113 residues in SIVmac239 CA [15]. Therefore, it was possible that amino acid substitutions such as P38S (corresponding to P37S in SIVsm and SIVmac239 CAs) and L109V (corresponding to V108 in SIVmac239 CA) in LSDQ CA might enhance its TRIM5-resistance. The β-hairpin domain in retroviral CAs is also an important determinant for evasion from TRIM5α-restriction [18,25,27] (Fig. 1C). Based on these considerations, we introduced various amino acid substitutions into the MN4/LSDQgtu CA (Table 1) to increase TRIM5α-resistance, hopefully up to the SIVmac239 CA level. Resultant proviral clones were tested for their growth abilities in a RhM cell line M1.3S. However, our extensive attempts to obtain biologically active CAs, potentially more resistant to macaque TRIM5 proteins than MN4/LSDQgtu CA, were unsuccessful so far (Table 1). Thus, some mutation(s) and/or combination(s) of mutations in CA other than those in Table 1 may be necessary to confer full resistance to TRIM5α on the HIV-1mt.

3.3. HIV-1mt clones carrying LSDQ/LNEIE CA replicate well in RhM PBMCs

To compare the effects of a different spectrum of mutations in CAs on viral growth potential, we examined LSDQ+4gtu and LNEIE+4gtu for their replication in RhM cells. In M1.3S cells (*TRIM5α*$^{TFP/TFP}$) [36], LSDQ+4gtu replicated slightly better than LNEIE+4gtu (Fig. 3A). In PBMCs prepared from four RhM individuals (*TRIM5α*$^{TFP/Q}$), LSDQ+4gtu grew better (Fig. 3B, upper panel) than or similarly to LNEIE+4gtu (Fig. 3B, lower panel). Next, to compare the competence of the CAs to that of SIVmac239 CA in terms of multi-cycle virus replication in RhM PBMCs, we newly constructed a proviral HIV-1mt clone carrying SIVmac239 CA. Because insertion of the entire CA-coding sequence of SIVmac into the corresponding region of HIV-1 genome was lethal, we generated a new Gag clone (SCA) exactly as previously reported for stHIV-1$_{SCA}$ [16,17] (Fig. 4A), and then made a proviral clone designated SCA+4gtu as described to construct LSDQ+4gtu and LNEIE+4gtu (Fig. 2A) for infection experiments. Proviral clone SCA was more replication-competent than LSDQ [15] (~3-fold) as determined in feline CRFK cells stably expressing RhM-TRIM5α (*TRIM5α*$^{TFP/TFP}$), but showed a lower titer (~2-fold–4-fold) in CRFK-naïve cells and TZM-bl indicator cells relative to LSDQ (our unpublished results). As shown in Fig. 4B, while LSDQ+4gtu grew better than SCA+4gtu in all four PBMC preparations tested (*TRIM5α*$^{TFP/Q}$), LNEIE+4gtu did so in two preparations (PBMCs from RhMs 610 and 611). In these two PBMC preparations, LSDQ+4gtu and LNEIE+4gtu grew similarly well. In the other two preparations, of note, LSDQ+4gtu grew better than LNEIE+4gtu (PBMCs from RhMs 599 and 609 in Fig. 4B). It remains to be elusive whether the observed difference in growth potentials in some PBMC preparations of the two clones are attributable to TRIM5α-restriction, viral fitness (infectivity of LNEIE determined in TZM-bl indicator cells relative to that of LSDQ was 0.72 on average), unknown cellular factor(s), and/or cellular physiological state/environments.

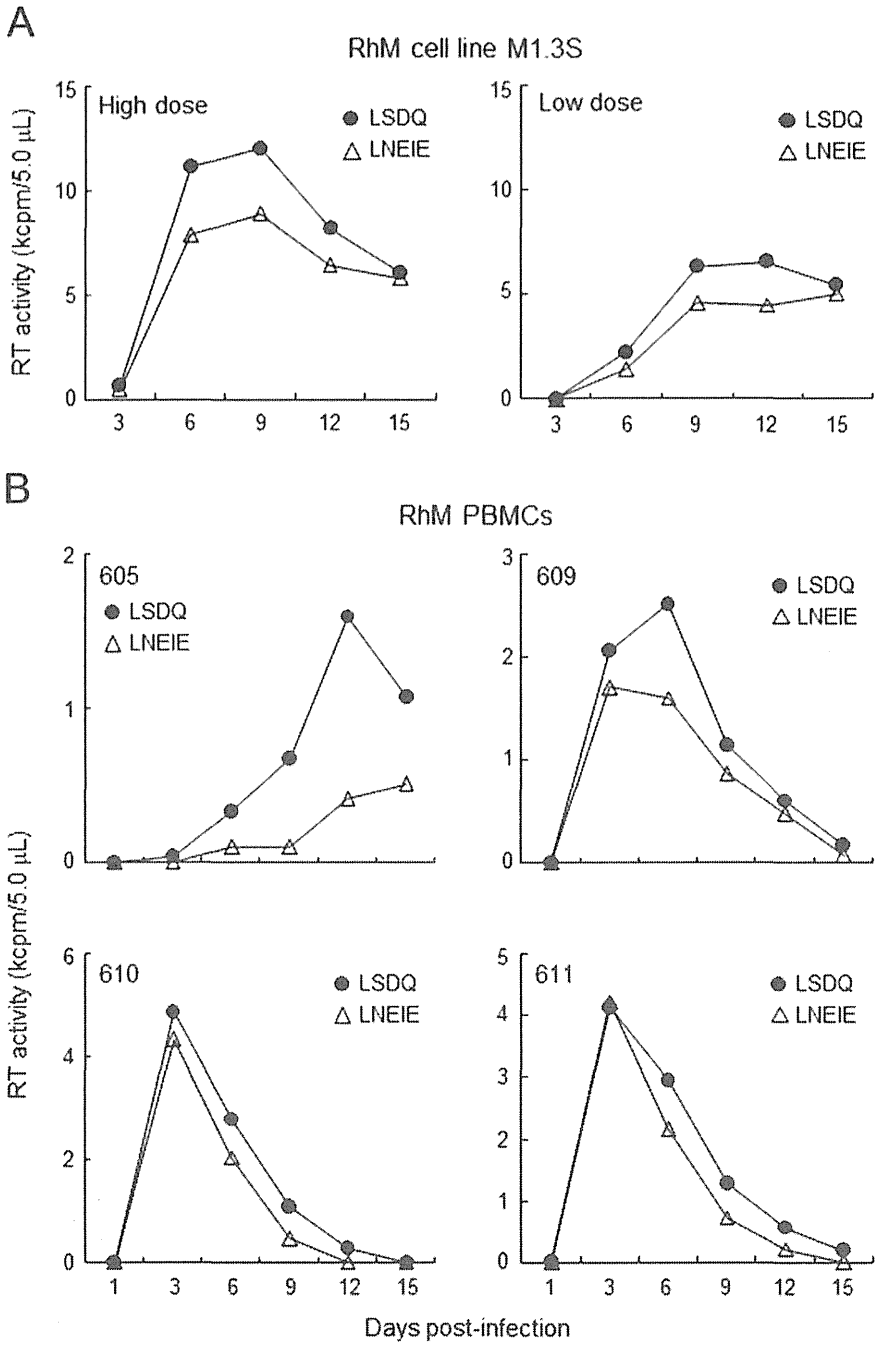

Fig. 3. Growth kinetics of two HIV-1mt clones with a distinct CA in RhM cells. Input viruses were prepared from 293T cells transfected with the indicated clones, and viral replication was monitored by RT activity released into the culture supernatants. LSDQ, LSDQ+4gtu; LNEIE, LNEIE+4gtu. (A) Infection of M1.3S cells (*TRIM5α*$^{TFP/TFP}$). Cells (2.0×10^5) were infected with equal virus amounts (High dose, 5.0×10^5 RT units; Low dose, 5.0×10^4 RT units). (B) Infection of PBMCs from four RhM individuals (*TRIM5α*$^{TFP/Q}$). Equal amounts of viruses were spin-infected into the PBMC preparations. Infection conditions were as follows: 2.4×10^6 RT units/1.0×10^6 cells for monkey 605; 4.0×10^6 RT units/2.0×10^6 cells for monkeys 609, 610, and 611.

4. Discussion

In this study, we performed side by side comparative analyses of the TRIM5-resistance/growth ability in RhM cells of HIV-1mt viruses carrying distinct CAs (LSDQ and LNEIE in Fig. 1) that are resistant to RhM TRIM5α [15,16]. LSDQ and LNEIE CAs exhibited various degrees of susceptibility to macaque TRIM5 proteins, and the former was generally more resistant to TRIM5-restriction than the latter in our TRIM5-overexpression system (Fig. 2). However, growth potentials of HIV-1mt viruses carrying LSDQ or LNEIE CA were similar in some preparations of RhM PBMCs, and varied among PBMCs from RhM individuals with *TRIM5*$^{TFP/Q}$ (Figs. 3 and 4). These results may only reflect a low endogenous expression level of TRIM5 proteins in PBMCs relative to that in cells infected with recombinant SeVs. The expression levels of TRIM5 proteins in various cells, however, can not be measured as yet due to the lack of appropriate anti-macaque

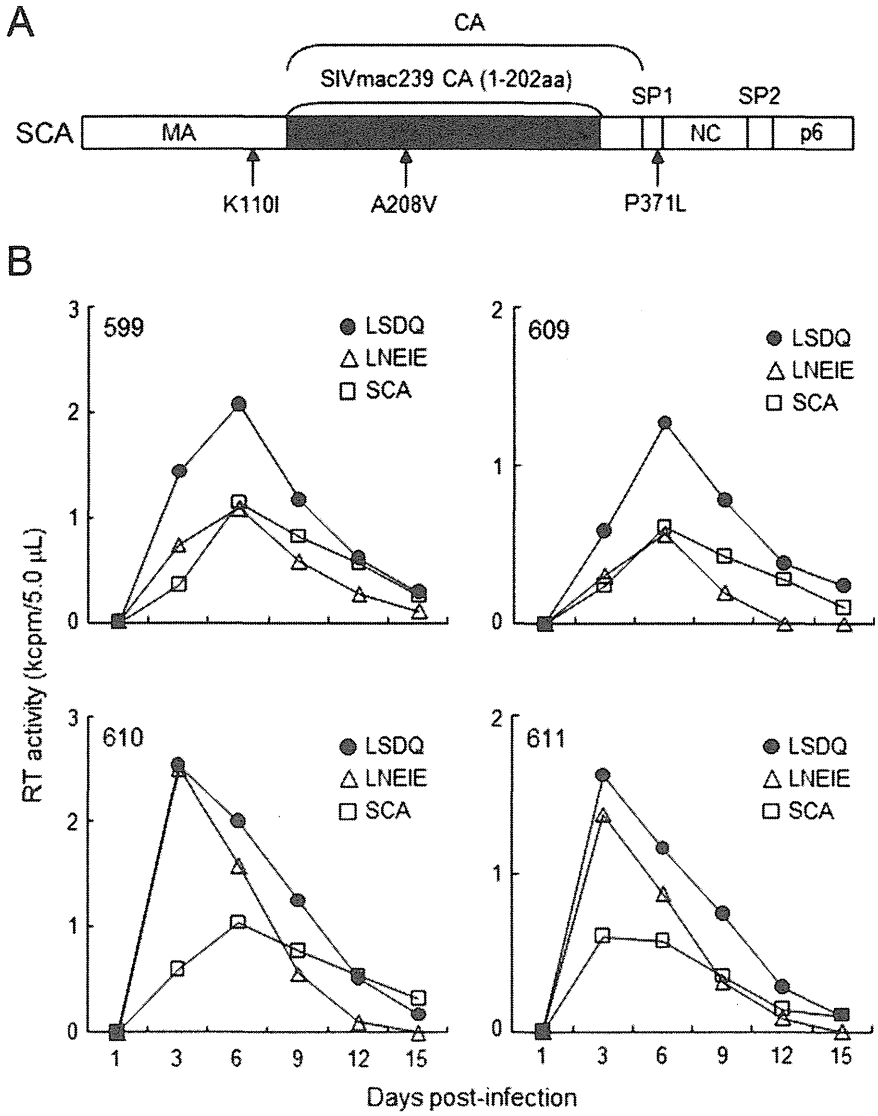

Fig. 4. Growth kinetics of various HIV-1mt clones with a distinct CA in RhM PBMCs. (A) Gag-coding region of pSCA. White and black areas show sequences from HIV-1_{NL4-3} and SIVmac239, respectively. Mutations introduced are indicated. MA, matrix; SP1, spacer peptide 1; NC, nucleocapsid; SP2, spacer peptide 2. (B) Infection of PBMCs from four RhM individuals (*TRIM5α*$^{TFP/Q}$). Input viruses were prepared from 293T cells transfected with the indicated clones, and equal amounts of viruses were spin-infected into the PBMCs. Infection conditions were as follows: 2.4 × 10^6 RT units/2.0 × 10^6 cells for monkey 599; 1.2 × 10^6 RT units/1.0 × 10^6 cells for monkeys 609, 610, and 611. Viral replication was monitored by RT activity released into the culture supernatants. LSDQ, LSDQ+4gtu; LNEIE, LNEIE+4gtu; SCA, SCA+4gtu.

TRIM5 antibodies. Alternatively, the above results suggest that overcoming TRIM5-restriction may not be enough for maximal virus growth of the HIV-1mt clones in RhM cells. Thus, a new generation of HIV-1mt clones that replicate constantly well in PBMCs from any RhM individuals like SIVmac239 would be necessary to establish the HIV-1-infected RhM model system. Of similar importance, detailed biological and structural analyses of the interaction between LSDQ/LNEIE CA and macaque TRIM5 proteins would contribute to better understand the underlying molecular mechanism for HIV-1 restriction by the proteins.

We previously suggested that R98S in HIV-1mt CA may be a key residue to circumvent macaque TRIM5α-restriction [15], since the corresponding residues in SIVsm and SIVmac239 CAs have been shown to contribute to the alteration of TRIM5α-susceptibility [25,30,35]. The coincidence of four amino acid residues important for evasion of RhM TRIM5-restriction in two independent studies on HIV-1 [15] and SIV [25] (L93, S97, D109, Q113 for SIVmac239 CA and L94, S98, D110, Q114 for HIV-1mt CA as described above) has raised a possible involvement of some specific amino acids in the TRIM5-regulation. However, comparative analysis of LSDQ and LNEIE clones here suggests that combinations of mutations in an appropriate context in CA rather than individual residues are critical for efficient escape from TRIM5α-restriction. As TRIM5α has evolved to target diverse retroviral CAs by flexibility of its B30.2/SPRY domain [7-9,12], HIV-1 can, in turn, gain RhM TRIM5α-resistance

through several distinct CAs with different amino acid sequences and/or CA surface patterns.

Conflict of interest

The authors declare that they have no conflict of interest.

Acknowledgments

We thank Ms. Kazuko Yoshida for editorial assistance. This study was supported in part by a grant from the Ministry of Health, Labor and Welfare of Japan (Research on HIV/AIDS project no. H24-005).

References

[1] Kratovac Z, Virgen CA, Bibollet-Ruche F, Hahn BH, Bieniasz PD, Hatziioannou T. Primate lentivirus capsid sensitivity to TRIM5 proteins. J Virol 2008;82:6772–7.

[2] Perron MJ, Stremlau M, Song B, Ulm W, Mulligan RC, Sodroski J. TRIM5alpha mediates the postentry block to N-tropic murine leukemia viruses in human cells. Proc Natl Acad Sci U S A 2004;101:11827–32.

[3] Song B, Javanbakht H, Perron M, Park DH, Stremlau M, Sodroski J. Retrovirus restriction by TRIM5alpha variants from old world and new world primates. J Virol 2005;79:3930–7.

[4] Stremlau M, Owens CM, Perron MJ, Kiessling M, Autissier P, Sodroski J. The cytoplasmic body component TRIM5alpha restricts HIV-1 infection in old world monkeys. Nature 2004;427:848–53.

[5] Yap MW, Nisole S, Lynch C, Stoye JP. Trim5alpha protein restricts both HIV-1 and murine leukemia virus. Proc Natl Acad Sci U S A 2004;101:10786–91.

[6] Ylinen LM, Keckesova Z, Wilson SJ, Ranasinghe S, Towers GJ. Differential restriction of human immunodeficiency virus type 2 and simian immunodeficiency virus SIVmac by TRIM5alpha alleles. J Virol 2005;79:11580–7.

[7] Biris N, Tomashevski A, Bhattacharya A, Diaz-Griffero F, Ivanov DN. Rhesus monkey TRIM5α SPRY domain recognizes multiple epitopes that span several capsid monomers on the surface of the HIV-1 mature viral core. J Mol Biol 2013;425:5032–44.

[8] Biris N, Yang Y, Taylor AB, Tomashevski A, Guo M, Hart PJ, et al. Structure of the rhesus monkey TRIM5α PRYSPRY domain, the HIV capsid recognition module. Proc Natl Acad Sci U S A 2012;109:13278–83.

[9] Ganser-Pornillos BK, Chandrasekaran V, Pornillos O, Sodroski JG, Sundquist WI, Yeager M. Hexagonal assembly of a restricting TRIM5α protein. Proc Natl Acad Sci U S A 2011;108:534–9.

[10] Sebastian S, Luban J. TRIM5alpha selectively binds a restriction-sensitive retroviral capsid. Retrovirology 2005;2:40.

[11] Stremlau M, Perron M, Lee M, Li Y, Song B, Javanbakht H, et al. Specific recognition and accelerated uncoating of retroviral capsids by the TRIM5alpha restriction factor. Proc Natl Acad Sci U S A 2006;103:5514–9.

[12] Yang H, Ji X, Zhao G, Ning J, Zhao Q, Aiken C, et al. Structural insight into HIV-1 capsid recognition by rhesus TRIM5α. Proc Natl Acad Sci U S A 2012;109:18372–7.

[13] Hatziioannou T, Evans DT. Animal models for HIV/AIDS research. Nat Rev Microbiol 2012;10:852–67.

[14] Nomaguchi M, Doi N, Fujiwara S, Adachi A. Macaque-tropic HIV-1 derivatives: a novel experimental approach to understand viral replication and evolution in vivo. In: Chang Theresa Li-Yun, editor. HIV-host interactions; 2011. p. 325–48. InTech, Rijeka, Croatia, http://www.intechopen.com/books/hiv-host-interactions/macaque-tropic-hiv-1-derivatives-a-novel-experimental-approach-to-understand-viral-replication-and-e.

[15] Nomaguchi M, Yokoyama M, Kono K, Nakayama EE, Shioda T, Doi N, et al. Generation of rhesus macaque-tropic HIV-1 clones that are resistant to major anti-HIV-1 restriction factors. J Virol 2013;87:11447–61.

[16] Soll SJ, Wilson SJ, Kutluay SB, Hatziioannou T, Bieniasz PD. Assisted evolution enables HIV-1 to overcome a high TRIM5α-imposed genetic barrier to rhesus macaque tropism. PLoS Pathog 2013;9:e1003667.

[17] Hatziioannou T, Princiotta M, Piatak Jr M, Yuan F, Zhang F, Lifson JD, et al. Generation of simian-tropic HIV-1 by restriction factor evasion. Science 2006;314:95.

[18] Kono K, Song H, Yokoyama M, Sato H, Shioda T, Nakayama EE. Multiple sites in the N-terminal half of simian immunodeficiency virus capsid protein contribute to evasion from rhesus monkey TRIM5α-mediated restriction. Retrovirology 2010;7:72.

[19] O'Doherty U, Swiggard WJ, Malim MH. Human immunodeficiency virus type 1 spinoculation enhances infection through virus binding. J Virol 2004;74:10074–80.

[20] Bichel K, Price AJ, Schaller T, Towers GJ, Freund SM, James LC. HIV-1 capsid undergoes coupled binding and isomerization by the nuclear pore protein NUP358. Retrovirology 2013;10:81.

[21] Hatziioannou T, Cowan S, Von Schwedler UK, Sundquist WI, Bieniasz PD. Species-specific tropism determinants in the human immunodeficiency virus type 1 capsid. J Virol 2004;78:6005–12.

[22] Kamada K, Igarashi T, Martin MA, Khamsri B, Hatcho K, Yamashita T, et al. Generation of HIV-1 derivatives that productively infect macaque monkey lymphoid cells. Proc Natl Acad Sci U S A 2006;103:16959–64.

[23] Kuroishi A, Saito A, Shingai Y, Shioda T, Nomaguchi M, Adachi A, et al. Modification of a loop sequence between alpha-helices 6 and 7 of virus capsid (CA) protein in a human immunodeficiency virus type 1 (HIV-1) derivative that has simian immunodeficiency virus (SIVmac239) vif and CA alpha-helices 4 and 5 loop improves replication in cynomolgus monkey cells. Retrovirology 2009;6:70.

[24] Lin TY, Emerman M. Determinants of cyclophilin A-dependent TRIM5 alpha restriction against HIV-1. Virology 2008;379:335–41.

[25] McCarthy KR, Schmidt AG, Kirmaier A, Wyand AL, Newman RM, Johnson WE. Gain-of-sensitivity mutations in a Trim5-resistant primary isolate of pathogenic SIV identify two independent conserved determinants of Trim5α specificity. PLoS Pathog 2013;9:e1003352.

[26] Nomaguchi M, Yokoyama M, Kono K, Nakayama EE, Shioda T, Saito A, et al. Gag-CA Q110D mutation elicits TRIM5-independent enhancement of HIV-1mt replication in macaque cells. Microbes Infect 2013;15:56–65.

[27] Ohkura S, Goldstone DC, Yap MW, Holden-Dye K, Taylor IA, Stoye JP. Novel escape mutants suggest an extensive TRIM5α binding site spanning the entire outer surface of the murine leukemia virus capsid protein. PLoS Pathog 2011;7:e1002011.

[28] Owens CM, Song B, Perron MJ, Yang PC, Stremlau M, Sodroski J. Binding and susceptibility to postentry restriction factors in monkey cells are specified by distinct regions of the human immunodeficiency virus type 1 capsid. J Virol 2004;78:5423–37.

[29] Pacheco B, Finzi A, Stremlau M, Sodroski J. Adaptation of HIV-1 to cells expressing rhesus monkey TRIM5α. Virology 2010;408:204–12.

[30] Kirmaier A, Wu F, Newman RM, Hall LR, Morgan JS, O'Connor S, et al. TRIM5 suppresses cross-species transmission of a primate immunodeficiency virus and selects for emergence of resistant variants in the new species. PLoS Biol 2010;8:e1000462.

[31] Newman RM, Hall L, Connole M, Chen GL, Sato S, Yuste E, et al. Balancing selection and the evolution of functional polymorphism in Old World monkey TRIM5alpha. Proc Natl Acad Sci U S A 2006;103:19134–9.

[32] Wilson SJ, Webb BL, Ylinen LM, Verschoor E, Heeney JL, Towers GJ. Independent evolution of an antiviral TRIMCyp in rhesus macaques. Proc Natl Acad Sci U S A 2008;105:3557–62.

[33] Price AJ, Marzetta F, Lammers M, Ylinen LM, Schaller T, Wilson SJ, et al. Active site remodeling switches HIV specificity of antiretroviral TRIMCyp. Nat Struct Mol Biol 2009;16:1036–42.

[34] Ylinen LM, Price AJ, Rasaiyaah J, Hué S, Rose NJ, Marzetta F, et al. Conformational adaptation of Asian macaque TRIMCyp directs lineage specific antiviral activity. PLoS Pathog 2010;6:e1001062.
[35] Wu F, Kirmaier A, Goeken R, Ourmanov I, Hall L, Morgan JS, et al. TRIM5 alpha drives SIVsmm evolution in rhesus macaques. PLoS Pathog 2013;9:e1003577.
[36] Doi N, Fujiwara S, Adachi A, Nomaguchi M. Rhesus M1.3S cells suitable for biological evaluation of macaque-tropic HIV/SIV clones. Front Microbiol 2011;2:115.
[37] von Schwedler UK, Stray KM, Garrus JE, Sundquist WI. Functional surfaces of the human immunodeficiency virus type 1 capsid protein. J Virol 2003;77:5439–50.
[38] Nomaguchi M, Doi N, Fujiwara S, Saito A, Akari H, Nakayama EE, et al. Systemic biological analysis of the mutations in two distinct HIV-1mt genomes occurred during replication in macaque cells. Microbes Infect 2013;15:319–28.

Journal of Infectious Diseases Advance Access published August 6, 2014

MAJOR ARTICLE

Epigenetic Repression of Interleukin 2 Expression in Senescent CD4$^+$ T Cells During Chronic HIV Type 1 Infection

Kaori Nakayama-Hosoya,[1,2] Takaomi Ishida,[3] Ben Youngblood,[5] Hitomi Nakamura,[1,2] Noriaki Hosoya,[1,2] Michiko Koga,[1] Tomohiko Koibuchi,[4] Aikichi Iwamoto,[1,2,3,4] and Ai Kawana-Tachikawa[1]

[1]Division of Infectious Diseases, Advanced Clinical Research Center, [2]International Research Center for Infectious Diseases, [3]Research Center for Asian Infectious Diseases, and [4]Department of Infectious Diseases and Applied Immunology, IMSUT Hospital, Institute of Medical Science, University of Tokyo, Japan; and [5]Department of Microbiology and Immunology, Emory University School of Medicine, Atlanta, Georgia

The molecular mechanisms for *IL2* gene–specific dysregulation during chronic human immunodeficiency virus type 1 (HIV-1) infection are unknown. Here, we investigated the role of DNA methylation in suppressing interleukin 2 (IL-2) expression in memory CD4$^+$ T cells during chronic HIV-1 infection. We observed that CpG sites in the *IL2* promoter of CD4$^+$ T cells were fully methylated in naive CD4$^+$ T cells and significantly demethylated in the memory populations. Interestingly, we found that the memory cells that had a terminally differentiated phenotype and expressed CD57 had increased *IL2* promoter methylation relative to less differentiated memory cells in healthy individuals. Importantly, early effector memory subsets from HIV-1–infected subjects expressed high levels of CD57 and were highly methylated at the *IL2* locus. Furthermore, the increased CD57 expression on memory CD4$^+$ T cells was inversely correlated with IL-2 production. These data suggest that DNA methylation at the *IL2* locus in CD4$^+$ T cells is coupled to immunosenescence and plays a critical role in the broad dysfunction that occurs in polyclonal T cells during HIV-1 infection.

Keywords. HIV-1; CD4$^+$ T-cell dysfunction; repression of IL-2 expression; DNA methylation; T-cell differentiation; immunosenescence.

During chronic human immunodeficiency virus type 1 (HIV-1) infection, CD4$^+$ T cells undergo cell-intrinsic phenotypic and functional impairments that are coupled to increased pathogenesis. These phenotypic changes include elevated levels of expression of activation, exhaustion, and senescent markers [1–5]. We have previously reported reduction in the expression of specific cytokines by T cells in HIV-1 noncontrollers, which is associated with activation/exhaustion status in both CD4$^+$ and CD8$^+$ memory T cells [6]. It has also been observed that both HIV-1-specific CD4$^+$ and CD8$^+$ T cells are less functional, with a particular impairment in interleukin 2 (IL-2) transcriptional expression, in individuals with disease progression, compared with long-term nonprogressors [7–10]. These data suggest that loss of function in T cells is, in part, due to gene-specific transcriptional dysregulation that is acquired during chronic HIV-1 infection. However, molecular mechanisms underlying the gene-specific reduction in expression have not been elucidated.

Epigenetic mechanisms of transcriptional regulation are critical for tissue and gene-specific transcript expression. Recently, it has become clear that epigenetic marks, such as DNA methylation and chromatin modification, modulate helper T-cell lineage commitment and function [11–14]. Furthermore, detailed analysis of epigenetic modification at the PD-1 locus in both mouse and human T cells indicates that the DNA methylation program modulates memory T-cell quality during persistent viral infection [15, 16]. Additionally, DNA demethylation at the promoter/enhancer region near the transcriptional start site of several genes coding

Received 16 February 2014; accepted 25 June 2014.

Correspondence: Ai Kawana-Tachikawa, Division of Infectious Diseases, Advanced Clinical Research Center, Institute of Medical Science, University of Tokyo, 4-6-1 Shirokanedai, Minato-ku, Tokyo 108-8639, Japan (aikawana@ims.u-tokyo.ac.jp).

The Journal of Infectious Diseases

DOI: 10.1093/infdis/jiu376

for cytokines, including *IL2*, occurs after T-cell activation [17–19]. However, the role of epigenetic reprogramming of the *IL2* promoter in dysfunctional T cells during chronic HIV-1 infection has not been examined.

In the present study, we evaluated DNA methylation at the promoter/enhancer region of *IL2* in $CD4^+$ and $CD8^+$ T cells from HIV-1–infected noncontrollers with suppressed IL-2 expression. We also measured *IL2* promoter DNA methylation in T-cell subsets from HIV-1–uninfected donors to gain further insight into the link between changes in DNA methylation and downregulation of IL-2 expression. Finally, we investigated the relationship between *IL2* promoter DNA methylation and CD57, a marker of replicative senescence on T cells and a characteristic feature of T cells in HIV-1–infected individuals.

MATERIALS AND METHODS

Study Population

Peripheral blood mononuclear cells (PBMCs) were obtained from 16 viremic controllers (median HIV-1 RNA level, 410 copies/mL; interquartile range, 105–613 copies/mL) and 19 noncontrollers (median HIV-1 RNA level, 71 000 copies/mL; interquartile range, 60 500–86 000 copies/mL). Untreated chronic and viremic controller donors with $CD4^+$ T-cell counts of approximately 400 cells/μL were identified and used for this study, to ensure that differences in downstream assays were not due to reduction in $CD4^+$ T-cell quantity. Seven individuals in the acute stage of HIV-1 infection (defined as ≤3 months after diagnosis) were recruited. Individuals showing symptoms of acute HIV-1 infection had a dramatic decline in viral load, and 8 individuals received combination antiretroviral therapy (cART) for prolonged period and were also included in this study (Table 1). Eleven HIV-1–seronegative individuals were enrolled in this study. All participants gave written informed consent. The study was approved by the institutional review boards of the Institute of Medical Science at the University of Tokyo (20-47-210521).

Cell Culture and T-Cell Stimulation

The frozen PBMCs were thawed and rested overnight before use in Roswell Park Memorial Institute 1640 medium supplemented with 10% heat-inactivated fetal calf serum. The PBMCs were stimulated with 2 μg/mL phytohemagglutinin-L (Roche) for 2.5 or 5 hours. Total messenger RNA (mRNA) was extracted 2.5 hours after stimulation for quantification of cytokine gene expression. Culture supernatants were harvested after 5 hours of stimulation for measurement of cytokine production. The human cytokine 25-plex antibody kit (Invitrogen) was used for measurement of the concentrations of multiple cytokines in the supernatant [6].

Quantification of mRNA by Real-Time Polymerase Chain Reaction (PCR)

Total RNA was extracted from the stimulated PBMCs, using an RNeasy Mini Kit (Qiagen), and was reverse transcribed with SuperScript III reverse transcriptase (Invitrogen), according to the manufacturer's protocol, with oligo dT primers. Quantitative reverse-transcription PCR was performed with the LightCycler TaqMan Master Kit and the LightCycler 2.0 capillary-based system, using the Universal ProbeLibrary (Roche). All samples were run in duplicate. The gene encoding succinate dehydrogenase complex subunit A (*SDHA*) was used as a reference gene [20].

$CD4^+$ and $CD8^+$ T-Cell Isolation

$CD4^+$ and $CD8^+$ T cells were isolated from PBMCs by magnetic cell separation–positive selection, using anti CD4 and CD8 antibody-conjugated beads (Miltenyi Biotic), according to the

Table 1. Characteristics of Study Subjects, by Group

	Controller (n = 16)	Noncontroller (n = 19)	Acutely Infected (n = 7)	cART Recipient (n = 8)	HIV-1-uninfected (n = 11)	P^a
Viral load, HIV-1 RNA copies/mL	410 (105–613)	71 000 (60 500–86 000)	230 000 (156 000–715 000)	Undetectable[b]	. . .	<.0001
T-cell count, cells/μL						
$CD4^+$	401 (377–468)	417 (329–442)	418 (300–492)	742 (606–795)	. . .	NS
$CD8^+$	893 (695–1103)	1302 (837–1760)	1262 (810–1668)	981 (809–1173)	. . .	.025
Age, y	34 (27–47)	39 (35–46)	41 (36–46)	44 (40–50)	38 (34–42)	NS
Duration after diagnosis, mo	50 (20–78)	29 (18–39)	≤3	82 (63–93)	. . .	NS
Treatment duration, mo	NA	NA	NA	60 (38–70)	. . .	. . .

Data are median (interquartile range).

Abbreviations: cART, combination antiretroviral therapy; HIV-1, human immunodeficiency virus type 1; NA, not applicable; NS, not significant.

[a] Data denote results of comparisons between controllers vs noncontrollers.

[b] Lower limit of detection (50 copies/mL), except a patient with 80 copies/mL.

manufacturer's instructions. The purity of each cell fraction was >95%, as determined by flow cytometry.

DNA Methylation Analysis

The analysis of DNA methylation was determined by bisulfate sequencing as previously described [21]. Briefly, genomic DNA from the purified $CD4^+$ T cells and $CD8^+$ T cells were treated with bisulfate, using the EpiTect Bisulfite Kit (Qiagen). Converted DNA (50 ng) was amplified by PCR with AccuPrime Taq DNA polymerase. The PCR was performed with the following locus-specific primers: 5′-GAGATAGGATTTTTTTAAGTGTTTTTAGGT-3′ and 5′-CATTAACCCACACTTAAATAATAACTCTAA-3′ for the *IL2* gene, 5′-GTTAAGAGGGAGAGAAGTAATTATAGATTT-3′ and 5′-AAATCTATAATTACTTCTCTCCCTCTTAAC-3′ for the tumor necrosis factor gene (*TNF*), and 5′-TGGAAAGAGGAGAGTGACAGAA-3′ and 5′-TTGGATGCTCTGGTCATCTTTA-3′ for the interferon γ gene (*IFNG*). The PCR products were cloned into the pGEM-T Easy vector system (Promega), and sequencing analysis was performed with at least 10 individual clones from each sample. All independent experiments were duplicated to avoid PCR amplification bias.

Antibodies

The following antibodies were used for flow cytometric analysis and cell sorting: CD57–fluorescein isothiocyanate (FITC), PD1-FITC, IL2-FITC, CD28–allophycocyanin (APC), CD45RA-APC, CCR7-phycoerythrin (PE)-Cy7, and CD3–Pacific blue (BD Pharmingen); CD27-FITC, CD8-PE, and CD3-peridinin chlorophyll protein-Cy5.5 (BD Biosciences); CD57-PE, CD45RA-APC-Cy7, CD4–Pacific blue, and CD8–Pacific blue (BioLegend); and CD4-APC-eFluor780 (eBioscience). Dead or dying cells were detected by staining with propidium iodide (Sigma).

Flow Cytometric Analysis and Cell Sorting of $CD4^+$ T-Cell Subsets

Multiparameter flow cytometry and cell sorting were performed with an Aria fluorescence-activated cell sorter (BD). Intracellular cytokine staining and surface staining were preformed as previously described [6]. For cell sorting, the sort logic was set by gating lymphocytes by forward scatter and side scatter and then gating on $CD3^+CD4^+$ cells. For methylation analysis of $CD4^+$ T-cell subsets, $CD4^+$ T cells were classified into 5 subsets based on expression of CD45RA, CCR7, CD27, and CD28: $CD45RA^+CCR7^+CD27^+CD28^+$ (naive), $CD45RA^-CCR7^+CD27^+CD28^+$ (central memory), $CD45RA^{+/-}CCR7^-CD27^+CD28^+$ (early effector memory), $CD45RA^{+/-}CCR7^-CD27^-CD28^+$ (intermediate effector memory), and $CD45RA^{+/-}CCR7^-CD27^-CD28^-$ (late effector memory). Memory $CD4^+$ T cells ($CD3^+CD4^+CD45RA^-$) were classified into further subsets based on expression of CD57. The purity of the sorted cell populations was >99%.

Statistical Analysis

GraphPad Prism5 software (GraphPad Software) was used for all statistical analysis. The Mann–Whitney *U* test and the Wilcoxon matched paired test were used for unpaired and paired comparisons, respectively. Correlation analysis was performed using Spearman rank correlation. Correction for multiple comparisons was assessed by calculating *q* values, the *P* value analogue of the false-discovery rate [22]. The level of significance for all analyses was set at a *P* value of <.05 and a *q* value of <0.2.

RESULTS

IL2 Gene Expression Is Impaired in HIV-1–Infected Noncontrollers During Chronic Infection

To elucidate a qualitative difference between T cells from viremic controllers and those from noncontrollers during chronic HIV-1 infection, we broadly assayed cytokine expression profiles from phytohemagglutinin-L (PHA)-stimulated PBMCs isolated from individuals with chronic HIV-1 infection. We found that IL-2, tumor necrosis factor α, interleukin 6, and interleukin 7 expression was significantly impaired in noncontrollers (Figure 1*A*). Because *IL2*, *TNF*, and *IL6* are early response genes that trigger sequential multiple immune responses and share some signaling pathways, we further examined mRNA expression of these genes at an earlier time point after PHA stimulation, to determine the hierarchy of reexpression. Importantly, the level of *IL2* mRNA expression was almost 4-fold higher in controllers relative to noncontrollers, whereas *TNF* and *IL6* mRNA expression levels were similar (Figure 1*B*). Furthermore, impaired *IL2* mRNA expression in noncontroller PBMCs was also observed after anti-CD3/CD28 stimulation (Supplementary Figure 1*A*). These data suggest that $CD4^+$ T cells in noncontrollers were qualitatively distinct in *IL2* gene regulation.

The *IL2* Promoter/Enhancer Region Is Hypermethylated in HIV-1–Infected Noncontrollers

Epigenetic modifications are a critical mechanism for stable gene expression. Specifically, acquired DNA methylation–mediated gene silencing can be maintained in a dividing population of cells [23–26]. The human *IL2* promoter contains 6 CpG sites within 1 kb immediately upstream of the transcriptional start site (Figure 2*A*) [18]. To investigate the role of DNA methylation in the restricted *IL2* expression in noncontrollers, we performed bisulfate sequencing to assess the level of DNA methylation at the individual CpG sites of the *IL2* promoter in $CD4^+$ and $CD8^+$ T cells isolated from HIV-1–infected individuals. The methylation frequency at all CpG sites in $CD4^+$ T cells was significantly higher in noncontrollers relative to that for $CD4^+$ T cells from controllers and HIV-1-uninfected individuals (Figure 2*B* and 2*C*). Notably, the difference was prominent in CpG site 1. In contrast, there was no significant

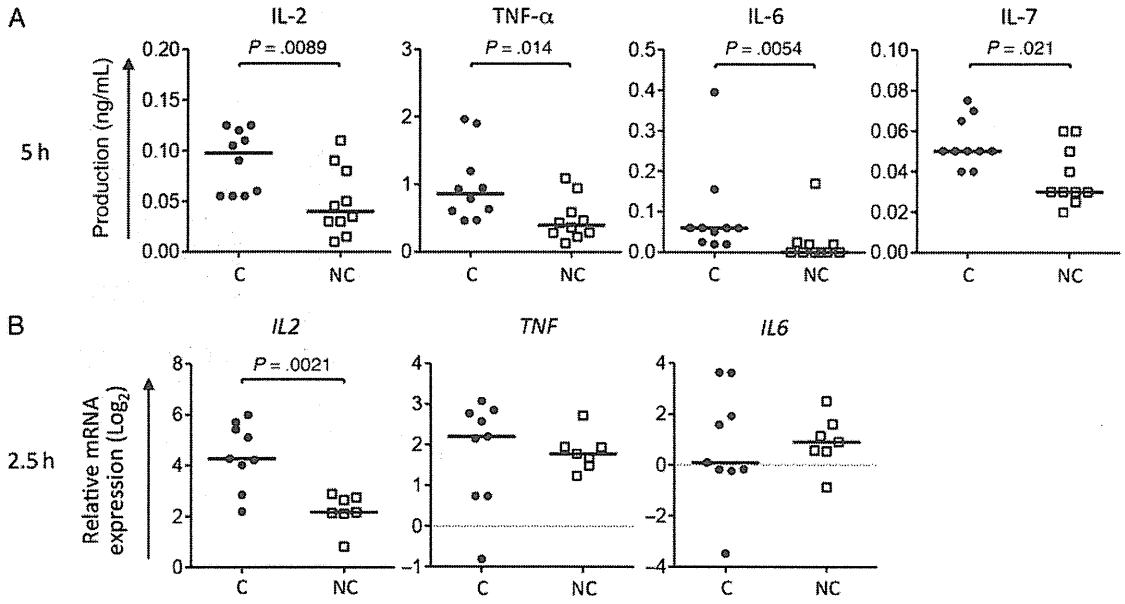

Figure 1. Cytokine transcription and protein expression profiling of phytohemagglutinin L (PHA)–stimulated peripheral blood mononuclear cells from individuals with chronic human immunodeficiency virus type 1 infection. Cytokine production (*A*) and messenger RNA (mRNA) expression of cytokines (*B*) after PHA stimulation. Data are normalized to the reference gene *SDHA* and are presented as fold change relative to unstimulated conditions. The horizontal bars indicate the median value. The Mann–Whitney *U* test was used for statistical analysis. Abbreviations: C, viremic controller; NC, noncontroller; IL-2, interleukin 2; IL-6, interleukin 6; IL-7, interleukin 7; TNF-α, tumor necrosis factor α.

difference in the methylation status of the *IL2* promoter in $CD8^+$ T cells between the groups (Figure 2*B* and Supplementary Figure 2*A*). It has previously been reported that *IFNG* and *TNF* promoters undergo methylation in aged people [27, 28]. Therefore, we sought to determine whether these promoters also acquired methylate promoters during chronic HIV-1 infection. Our bisulfite sequencing data indicate that there is not a significant difference in DNA methylation of the both *IFNG* and *TNF* promoter in $CD4^+$ and $CD8^+$ T cells between HIV-1 controllers and noncontrollers (Supplementary Figure 2*B* and 2*C*). To further determine whether the increase in methylation of the *IL2* promoter was coupled to a reduction in expression, we measured IL-2 expression in PHA-stimulated PBMCs and compared it to the *IL2* promoter methylation status in $CD4^+$ T cells. The DNA methylation status at CpG site 1 in $CD4^+$ T cells was inversely correlated to *IL2* mRNA expression and IL-2 production (Figure 2*D*). The inverse correlation was also observed when anti-CD3/CD28 was used as a stimulus (Supplementary Figure 1*B*). These data indicate that DNA hypermethylation at CpG site 1 in $CD4^+$ T cells is coupled to low IL-2 expression in noncontrollers during chronic HIV-1 infection.

$CD4^+$ T Cells From cART Recipients Have a Hypomethylated *IL2* Promoter

We next examined the DNA methylation status of the *IL2* promoter in $CD4^+$ T cells at different clinical stages of HIV-1 infection. We measured the methylation status of the *IL2* promoter in $CD4^+$ T cells from HIV-1–infected individuals with a high viral load in the acute stage of infection (Figure 2*E*). Surprisingly, the level of methylation of the *IL2* promoter in $CD4^+$ T cells from HIV-1–infected individuals in the acute stage of infection was similar to $CD4^+$ T cells from controllers and those from HIV-1-uninfected individuals. These data suggest that a high viral load itself does not affect the methylation status of the *IL2* locus.

We next sought to determine whether reduction of the HIV level in chronically infected individuals would result in demethylation of the *IL2* promoter. We performed a longitudinal analysis of *IL2* promoter methylation in $CD4^+$ T cells isolated from individuals before they received cART and after they achieved prolonged cART-mediated virus suppression. The subjects with prolonged viral suppression had recovery in $CD4^+$ T-cell counts, and, importantly, hypermethylation at CpG site 1 in the *IL2* locus before starting cART declined to normal levels after prolonged virus suppression in all individuals (Figure 2*F*). Indeed, the level of *IL2* promoter methylation in treated individuals was similar to the promoter methylation levels in HIV-1 controllers and uninfected individuals (Figure 2*E*). These data suggest that *IL2* promoter hypermethylation results from persistent high viral loads but is reversible after cART-mediated virus suppression.

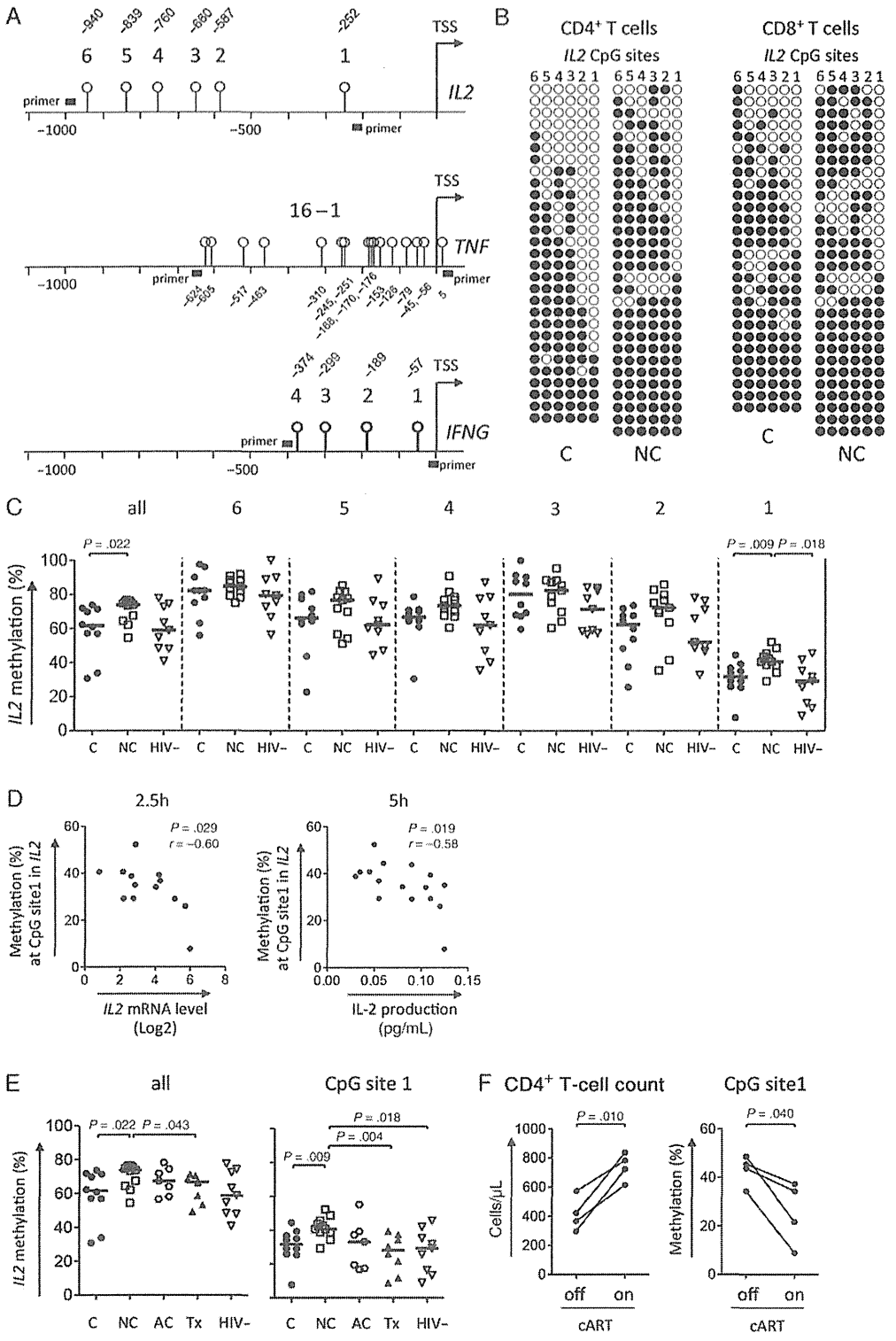

Figure 2. DNA methylation analysis of the *IL2* locus in human immunodeficiency virus type 1 (HIV-1)–infected individuals. *A*, Diagram of CpG position relative to the transcriptional start site of the *IL2, TNF,* and *IFNG* loci. *B*, Representative bisulfite sequencing DNA methylation analysis of the *IL2* locus in $CD4^+$ and $CD8^+$ T cells from viremic controllers and noncontrollers. Each line represents an individual clone picked for sequencing (filled circles, methylated cytosine; open circles, unmethylated cytosine). *C*, DNA methylation status of the *IL2* locus at CpG sites 1–6 in $CD4^+$ T cells from healthy and HIV-1–infected individuals. *D*, Correlation plot between methylation at CpG site 1 in $CD4^+$ T cells and interleukin 2 (IL-2) expression in peripheral blood mononuclear cells. *E*, DNA methylation status in all and at CpG site 1 in $CD4^+$ T cells at different clinical status in HIV-1 infection. *F*, Longitudinal change of methylation status at CpG site 1 and $CD4^+$ T-cell count in 4 subjects before and after combination antiretroviral therapy initiation. The Mann–Whitney *U* test (*C* and *E*) and the Wilcoxon matched paired test (*F*) were used for statistical analysis. Correlation coefficient and *P* values determined by the Spearman rank correlation test are shown in panel *D*. Abbreviations: AC, acute HIV-1 infection; C; controller, NC; noncontroller; Tx, treated with combination antiretroviral therapy; HIV-, HIV-1-uninfected.

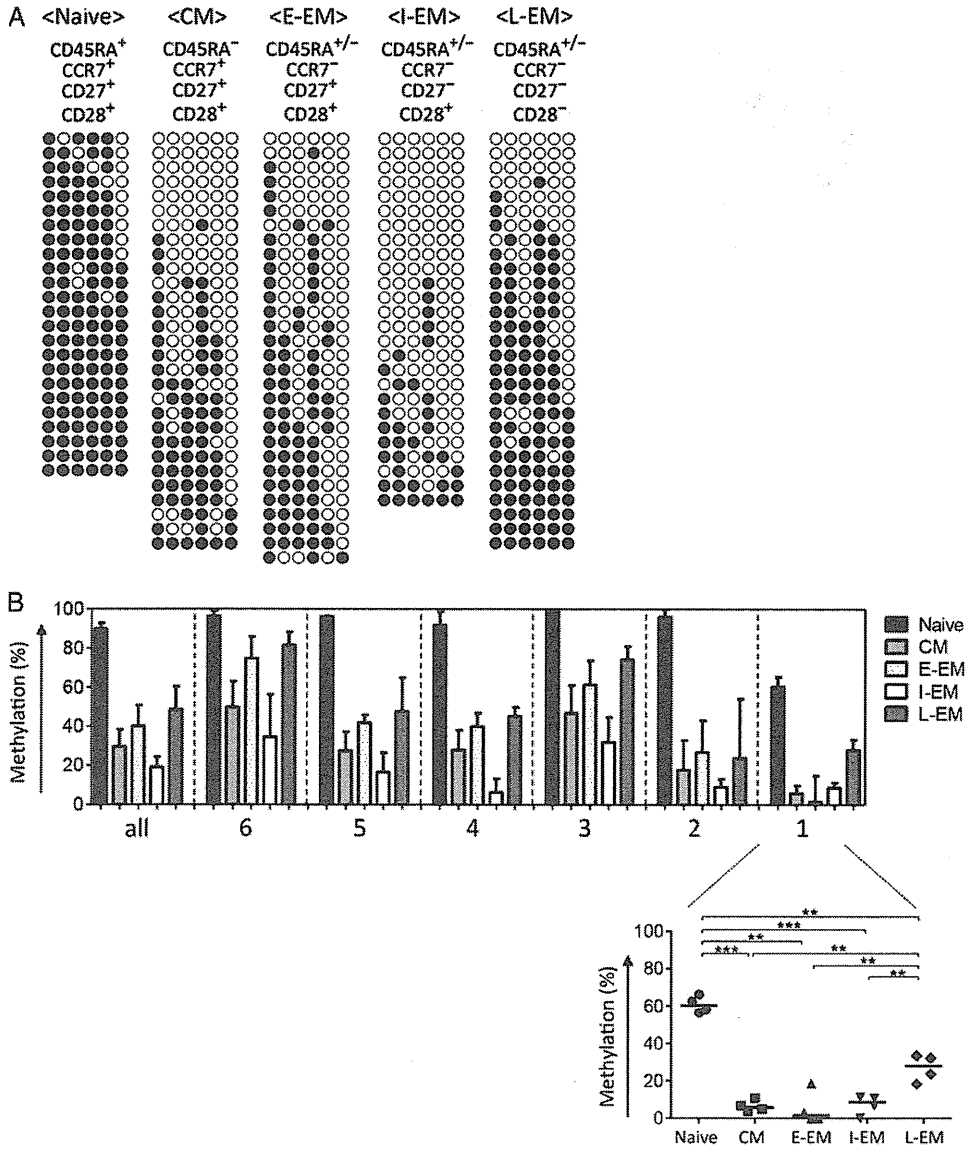

Figure 3. DNA methylation status of the *IL2* locus in different CD4+ T-cell subsets. *A*, Representative bisulfite sequencing DNA methylation analysis of the *IL2* locus in naive, central memory (CM), early effector memory (E-EM), intermediate effector memory (I-EM), and late effector memory (L-EM) CD4+ T-cell subsets, classified according to CD45RA, CCR7, CD27, and CD28 expression. *B*, Summary graph of DNA methylation status of the *IL2* locus in T-cell subsets in 4 individuals without HIV-1 infection. The paired *t* test was performed for statistical analysis. $^{**}P = .001–.01$, $^{***}P < .001$.

Phenotypically Senescent Memory CD4+ T Cells Have a Methylated *IL2* Promoter

Although the DNA methylation status of the *IL2* promoter/enhancer region in different CD4+ T cells in mice has been well characterized [17, 29, 30], the detailed profile of *IL2* promoter methylation in human CD4+ T cells has not been elucidated. Therefore, we sorted different CD4+ T-cell subsets in HIV-1-uninfected individuals on the basis of CD45RA, CCR7, CD27, and CD28 expression [31–33] and assessed the methylation status of the *IL2* promoter in each fraction (Figure 3). CpG sites 2–6 were fully methylated, and CpG site 1 was 60% methylated in naive CD4+ T cells (Figure 3*A* and 3*B*). In contrast, CpG sites 2–6 were >50% demethylated in all memory subsets (Figure 3*B*). Moreover, CpG site 1 was fully demethylated in central memory, early effector memory, and intermediate effector memory cell compartments (Figure 3*B*). Interestingly, all CpG sites, including site 1, were remethylated in late effector memory cells. Since signaling through CD28 has been shown to modify the epigenetic program of the *IL2* promoter in mice [30], we postulated that the *IL2* promoter may have an altered DNA methylation program in late effector memory subsets without CD28 expression.

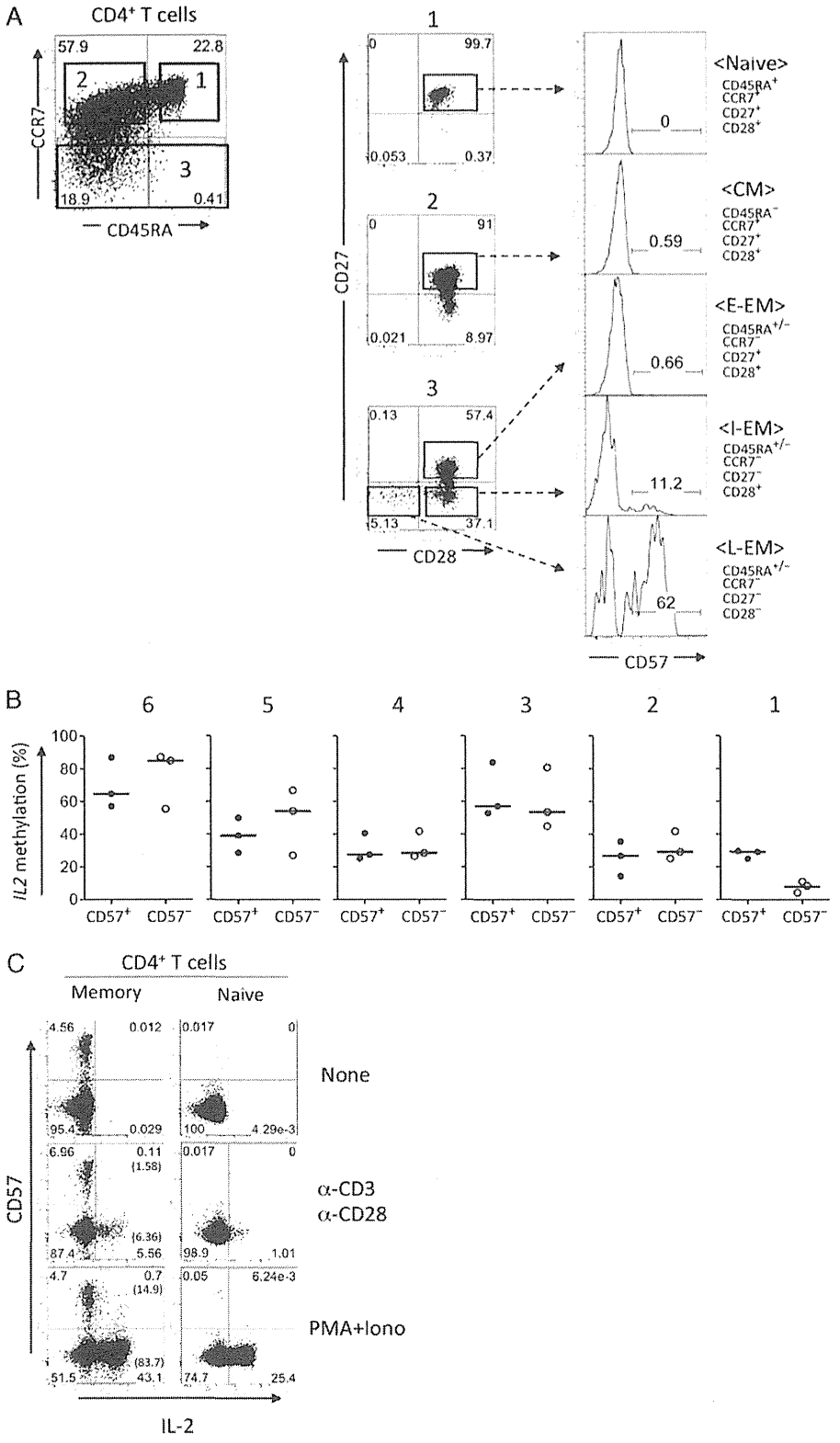

Figure 4. Analysis of CD57 expression and *IL2* locus DNA methylation in memory CD4+ T-cell subsets. *A*, Representative flow cytometric analysis of CD57 expression on CD4+ T-cell subsets classified by CD45RA, CCR7, CD27, and CD28 expression. *B*, Summary graph of the *IL2* locus DNA methylation status at CpG sites 1–6 in CD57+ and CD57− memory (CD45RA−) CD4+ T cells from 3 individuals without human immunodeficiency virus type 1 (HIV-1) infection. *C*, Flow cytometric analysis of CD57 and IL-2 expression after stimulation with α-CD3/CD28 and PMA/ionomycin in peripheral blood mononuclear cells from an HIV-1-uninfected individual. Values within brackets indicate the proportion of IL-2 secreting cells in CD57+ and CD57− cells. Abbreviations: CM, central memory; E-EM, early effector memory; I-EM, intermediate effector memory; L-EM, late effector memory.

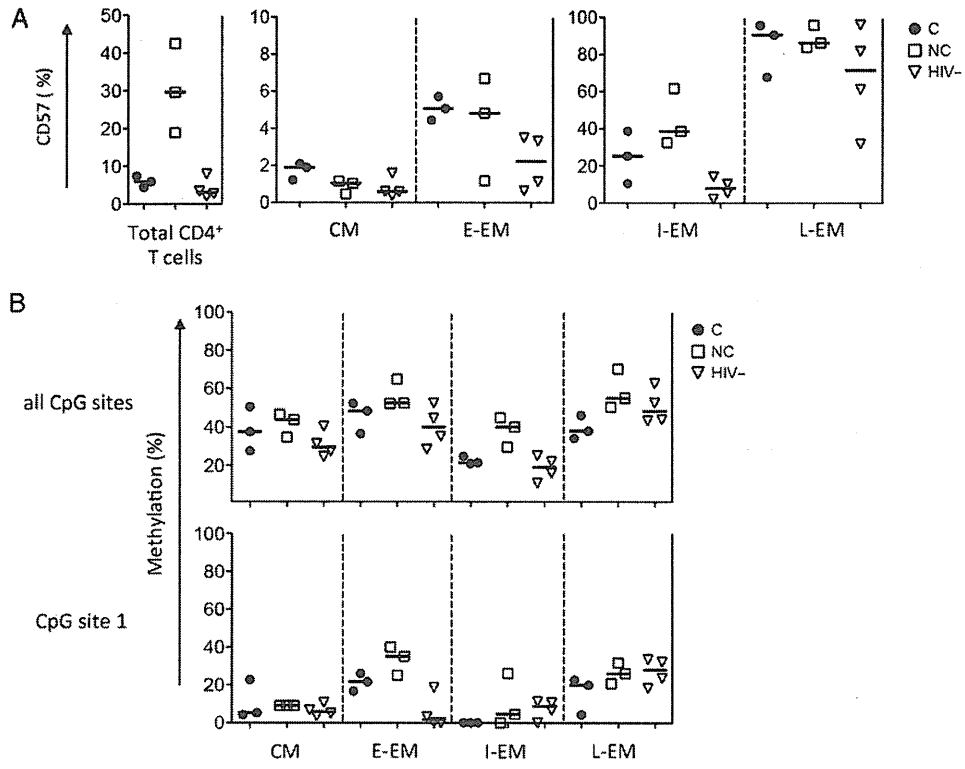

Figure 5. DNA methylation analysis of the *IL2* locus in memory CD4$^+$ T-cell subsets from individuals with chronic human immunodeficiency virus type 1 (HIV-1) infection. Summary graphs of CD57 expression level (*A*) and DNA methylation status of the *IL2* locus (*B*) in memory CD4$^+$ T-cell subsets. The memory subsets were defined by CD45RA, CCR7, CD27, and CD28 expression as shown in Figure 4*A*. Abbreviations: C, viremic controller; NC, noncontroller; HIV-, HIV-1-uninfected; CM, central memory; E-EM, early effector memory; I-EM, intermediate effector memory; L-EM, late effector memory.

It has also been reported that expression of CD57 is highly correlated with loss of CD28 expression in CD4$^+$ T cells [34–36] and is associated with replicative senescent T cells [34, 37, 38]. On the basis of these observations, we evaluated the association between CD57 expression and DNA methylation of the *IL2* promoter. We first analyzed CD57 expression in each CD4$^+$ T-cell subset. Naive, central memory, and early effector memory CD4$^+$ T cells from healthy individuals did not express CD57, while a significantly increased frequency of CD4$^+$ T-cell subsets with a more differentiated phenotype expressed CD57, with the highest level of expression observed on the late effector memory subset. We next assessed the DNA methylation status of the *IL2* promoter in CD57$^+$ and CD57$^-$ subsets of memory (CD45RA$^-$) CD4$^+$ T cells (Figure 4*B*). We found that CpG site 1 was more methylated in the CD57$^+$ subsets relative to the CD57$^-$ subsets. Importantly, IL-2 secretion in CD57-expressing memory CD4$^+$ T cells was 5-fold lower than IL-2 secretion in CD57$^-$ memory CD4$^+$ T cells even after strong T-cell stimulation with PMA/ionomycin (14.9% vs 83.7%; Figure 4*C*). These data indicate that CD57$^+$ cells among late effector memory CD4$^+$ T cells were remethylated at CpG site 1 of the *IL2* promoter, which was coupled to restricted IL-2 expression.

CD57$^+$CD4$^+$ T Cells in HIV-1–Infected Noncontrollers Have a Methylated *IL2* Promoter and Restricted IL-2 Expression

It has also been reported that HIV-1-specific CD57$^+$CD4$^+$ T cells have reduced IL-2 expression [35, 39]. Abnormal T-cell differentiation of polyclonal CD4$^+$ and CD8$^+$ T cells in HIV-1-infected individuals is associated with increased levels of CD57 expression [5, 35]. To determine whether the increased immune dysfunction in polyclonal memory T cells during chronic HIV-1 infection is associated with stable epigenetic programming of the memory pool, we measured DNA methylation of the *IL2* promoter in memory CD4$^+$ T-cell subsets from HIV-1–infected individuals. As previously reported [5, 35], the number of CD57$^+$ effector memory (early, intermediate, and late) CD4$^+$ T cells was higher in chronically infected individuals, compared with individuals without HIV infection (Figure 5*A*). We also observed an increase in methylation of the *IL2* promoter, not only in the late effector memory subset, but also in the less differentiated early effector memory and intermediate effector memory subsets from noncontrollers (Figure 5*B*). These data suggest that aberrant epigenetic modification at *IL2* promoter, coupled to CD57 expression, occurs at an early stage of CD4$^+$ T-cell differentiation during chronic HIV-1 infection.

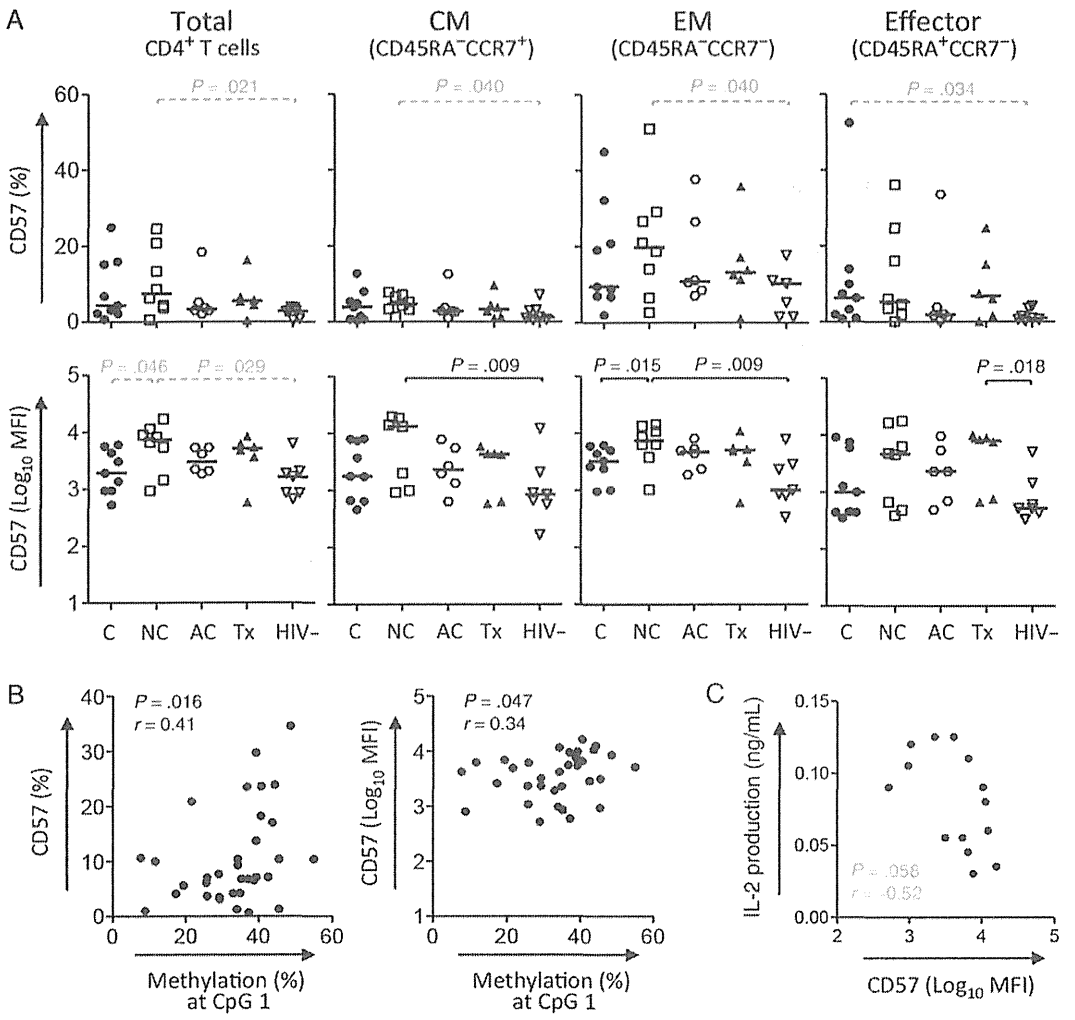

Figure 6. CD57 expression and methylation analysis of CpG site 1 in the *IL2* locus of CD4 memory T-cell subsets from individuals with human immunodeficiency virus type 1 (HIV-1) infection. *A*, Summary graph of CD57 expression level in each subset of $CD4^+$ T cells classified by CD45RA and CCR7. The Mann–Whitney *U* test was used for statistical analysis. *B*, Correlation plot of methylation at CpG site 1 vs CD57 expression in memory $CD4^+$ T cells. *C*, Correlation plot of methylation at CpG site 1 in $CD4^+$ T-cell vs IL-2 production in PHA-stimulated PBMCs. Correlation coefficient and *P* values in Spearman's rank correlation test are shown. *P* values less than .05 with $q > 0.2$ show in gray. Abbreviations: C, controller; NC, noncontroller; Ac, acute HIV-1 infection; Tx, treated with cART; HIV-, HIV-1-uninfected; CM, central memory; EM, effector memory.

We next measured the level of CD57 expression on individual $CD4^+$ T-cell subsets in all study groups (Figure 6*A*). Our data reveal that the frequency of $CD57^+$ cells was higher in noncontrollers than other groups and that the mean fluorescence intensity of CD57 expression on the total pool of memory $CD4^+$ T cells was significantly higher in noncontrollers.

Finally, we performed a correlation analysis between CD57 expression, DNA methylation of the *IL2* promoter, and IL-2 expression. A positive correlation was observed between CD57 expression and DNA methylation at CpG site 1 in the *IL2* promoter (Figure 6*B*). We also found a negative correlation between CD57 expression and IL-2 production in HIV-1–infected individuals (Figure 6*C*). Together, these data support a model whereby prolonged exposure of memory $CD4^+$ T cells to the chronic inflammatory environment in HIV-1 noncontrollers results in upregulation in CD57 expression and hypermethylation of the *IL2* promoter, ultimately resulting in senescence of polyclonal memory $CD4^+$ T cells.

DISCUSSION

Although many studies about T-cell immunopathogenesis during chronic HIV-1 infection have been reported, the molecular basis for T-cell dysfunction is not well understood. To better understand the mechanism for the broad decline in $CD4^+$ T-cell function during chronic HIV-1 infection, we performed

a combination of molecular and cellular assays that assessed the epigenetic profile of T cells relative to their ability to express cytokines in HIV-1 noncontrollers. Our results demonstrate that the CpG sites in the *IL2* promoter are highly methylated in $CD4^+$ T cells in noncontrollers and that the lower IL-2 expression is correlated with *IL2* promoter DNA methylation in $CD4^+$ T cells. Furthermore, DNA methylation was positively correlated with CD57 expression on memory $CD4^+$ T cells. To understand the relationship between $CD4^+$ T-cell quality and the *IL2* DNA methylation, we sorted $CD4^+$ T-cell subsets on the basis of differentiation and senescent markers and analyzed the methylation of CpG sites in the *IL2* locus. Naive $CD4^+$ T cells were fully methylated, and demethylation occurred at all CpG sites during T-cell differentiation, consistent with previous reports using mouse model systems [17, 19]. CpG sites were partially but significantly remethylated in terminally differentiated $CD4^+$ T cells in healthy individuals. We also found that $CD57^+$ cells, most of which possessed a terminally differentiated phenotype in HIV-uninfected individuals, were highly methylated at CpG site 1, compared with $CD57^-$ memory $CD4^+$ T cells. In contrast, the *IL2* promoter in memory $CD4^+$ T cells from HIV-1–infected noncontrollers was highly methylated. Further, the promoter was also methylated in less differentiated $CD57^+$ memory $CD4^+$ T cells. Taken together, our data suggest that loss of *IL2* expression in senescent $CD4^+$ T cells is regulated by DNA methylation during chronic HIV-1 infection.

Our results indicate that the genomic region proximal to CpG site 1 in the *IL2* promoter is important for transcriptional regulation of the gene. This regulatory region includes binding sites for critical transcription factors in the *IL2* promoter/enhancer region [18, 40, 41]. It has also been shown that the CpG site 1–specific methylation abrogates Oct-1/NFAT binding to the regulatory region and causes inhibition of *IL2* expression in Jurkat cells [18]. In the present study, we observed higher methylation in not only site 1 but all CpG sites in HIV-1 noncontrollers, suggesting that other CpG sites may be involved in *IL2* gene regulation by altering accessibility of chromatin and/or transcription factor binding.

IL-2 expression strongly depends on costimulatory signals through the CD28 superfamily of receptors during antigenic stimulation [40, 42]. It has been reported that the increase in histone acetylation and DNA demethylation at the *IL2* locus after T-cell receptor activation is impaired in the absence of CD28 costimulation [29, 30]. In this study, we observed increased levels of methylation of the *IL2* promoter only in terminally differentiated $CD4^+$ T cells without CD28 expression in HIV-1-uninfected individuals, supporting the idea that CD28 signaling plays an important role in DNA demethylation and/or remethylation of the *IL2* gene. However, we also observed DNA hypermethylation in early effector memory subsets with CD28 expression in HIV-1 noncontrollers, in which CD57 expression was abnormally elevated. In our experiments using HIV-1-uninfected subjects, CpG site 1 methylation was approximately 3-fold higher in $CD57^+$ versus $CD57^-$ memory $CD4^+$ T cells. Furthermore, we observed a positive correlation between CD57 expression in memory $CD4^+$ T cells and DNA methylation at CpG site 1 in the *IL2* promoter and also found a negative correlation between CD57 expression and IL-2 production in stimulated PBMCs. Taken together, our data indicate that CD57 engagement results in epigenetic modification of the *IL2* gene in a CD28-independent manner. The mechanism for gene regulation of CD28 and CD57 during the development of senescent T cells in the aged population remains unknown. Therefore, future studies should investigate molecular mechanisms underlying the relationship between the expression of IL-2 and these surface molecules. Of note, we observed no difference in *IL2* promoter DNA methylation in $CD8^+$ T cells. Meanwhile, it has been reported that IL-2 secretion in HIV-1-specific $CD8^+$ T cells was also impaired in progressors [7, 43]. Therefore, it is likely that mechanisms aside from DNA methylation regulate IL-2 expression. It will also be important for future studies to include analysis of epigenetic programs of effector molecules in HIV-1-specific T cells before and after cART initiation.

In the present study, we have identified epigenetic modification of the *IL2* promoter as a potential mechanism for the loss of IL-2 expression in $CD4^+$ T cells. This reprogramming of the *IL2* promoter may be coupled to the signaling events that also induce T-cell senescence during chronic HIV-1 infection. Individuals with chronic HIV-1 infection with a high viral load who maintained a certain $CD4^+$ T-cell count were recruited as noncontrollers, and individuals in late phase of HIV-1 infection and patients with AIDS were excluded in this study. Although there was no significant difference in $CD4^+$ T-cell count between controllers and noncontrollers in our cohort (by design), we observed DNA hypermethylation of the *IL2* locus in noncontrollers. In contrast, acutely infected individuals with a high viral load did not show the defect. These data suggest that $CD4^+$ T cells become senescent with loss of IL-2 expression before the decline in $CD4^+$ T-cell quantity if the immune system is persistently exposed persistently to high viral loads during chronic HIV-1 infection. Our data support the concept that early initiation of cART is a promising way to slow HIV-1 disease progression and immunosenescence.

Supplementary Data

Supplementary materials are available at *The Journal of Infectious Diseases* online (http://jid.oxfordjournals.org). Supplementary materials consist of data provided by the author that are published to benefit the reader. The posted materials are not copyedited. The contents of all supplementary data are the sole responsibility of the authors. Questions or messages regarding errors should be addressed to the author.

Notes

Acknowledgments. We thank all of the participants and clinical staff at the Research Hospital of the Institute of Medical Science, University of Tokyo, for their contributions.

Financial support. This work was supported by JSPS KAKENHI (grant 25293226 to A. K.-T.); the Ministry of Health, Labor, and Welfare of Japan (grants H24-AIDS-IPPAN-008 and H25-AIDS-IPPAN-007 to A. K.-T. and Research on International Cooperation in Medical Science, Research on Global Health Issues, and Health and Labor Science Research Grants H25-KOKUI-SITEI-001 to A. I.); Banyu Life Science Foundation International (grant to A. K.-T.); the Ministry of Education, Culture, Sports, Science and Technology (MEXT; contract 10005010 to A. I. and T. I., for the Program of Japan Initiative for Global Research Network on Infectious Diseases); and Global Centers of Excellence Program, MEXT (grant F06 to A. I.).

Potential conflicts of interest. A. K.-T. has received speaker's honoraria from ViiV Healthcare. A. I. has received grant support from Toyama Chemical, Astellas, ViiV Healthcare, MSD, and Baxter, through the University of Tokyo; and speaker's honoraria and payment for manuscript writing from Eiken Chemical, Astellas, Toyama Chemical, Torii Pharmaceutical, MSD, and Taisho Toyama Pharmaceutical. T. K. has received speaker's honoraria from Torii Pharmaceutical, MSD, ViiV Healthcare, Janssen Pharmaceutical, and AbbVie Inc. All other authors report no potential conflicts.

All authors have submitted the ICMJE Form for Disclosure of Potential Conflicts of Interest. Conflicts that the editors consider relevant to the content of the manuscript have been disclosed.

References

1. Appay V, Dunbar PR, Callan M, et al. Memory CD8+ T cells vary in differentiation phenotype in different persistent virus infections. Nat Med **2002**; 8:379–85.
2. Day CL, Kaufmann DE, Kiepiela P, et al. PD-1 expression on HIV-specific T cells is associated with T-cell exhaustion and disease progression. Nature **2006**; 443:350–4.
3. Kaufmann DE, Kavanagh DG, Pereyra F, et al. Upregulation of CTLA-4 by HIV-specific CD4+ T cells correlates with disease progression and defines a reversible immune dysfunction. Nat Immunol **2007**; 8: 1246–54.
4. Brenchley JM, Karandikar NJ, Betts MR, et al. Expression of CD57 defines replicative senescence and antigen-induced apoptotic death of CD8+ T cells. Blood **2003**; 101:2711–20.
5. Breton G, Chomont N, Takata H, et al. Programmed death-1 is a marker for abnormal distribution of naive/memory T cell subsets in HIV-1 infection. J Immunol **2013**; 191:2194–204.
6. Nakayama K, Nakamura H, Koga M, et al. Imbalanced production of cytokines by T cells associates with the activation/exhaustion status of memory T cells in chronic HIV type 1 infection. AIDS Res Hum Retroviruses **2012**; 28:702–14.
7. Betts MR, Nason MC, West SM, et al. HIV nonprogressors preferentially maintain highly functional HIV-specific CD8+ T cells. Blood **2006**; 107:4781–9.
8. Palmer BE, Boritz E, Wilson CC. Effects of sustained HIV-1 plasma viremia on HIV-1 Gag-specific CD4+ T cell maturation and function. J Immunol **2004**; 172:3337–47.
9. Ferrando-Martinez S, Casazza JP, Leal M, et al. Differential Gag-specific polyfunctional T cell maturation patterns in HIV-1 elite controllers. J Virol **2012**; 86:3667–74.
10. Potter SJ, Lacabaratz C, Lambotte O, et al. Preserved central memory and activated effector memory CD4+ T-cell subsets in human immunodeficiency virus controllers: an ANRS EP36 study. J Virol **2007**; 81:13904–15.
11. Wilson CB, Rowell E, Sekimata M. Epigenetic control of T-helper-cell differentiation. Nat Rev Immunol **2009**; 9:91–105.
12. Deaton AM, Webb S, Kerr AR, et al. Cell type-specific DNA methylation at intragenic CpG islands in the immune system. Genome Res **2011**; 21:1074–86.
13. Allan RS, Zueva E, Cammas F, et al. An epigenetic silencing pathway controlling T helper 2 cell lineage commitment. Nature **2012**; 487:249–53.
14. Lee GR, Kim ST, Spilianakis CG, Fields PE, Flavell RA. T helper cell differentiation: regulation by cis elements and epigenetics. Immunity **2006**; 24:369–79.
15. Youngblood B, Oestreich KJ, Ha SJ, et al. Chronic virus infection enforces demethylation of the locus that encodes PD-1 in antigen-specific CD8(+) T cells. Immunity **2011**; 35:400–12.
16. Youngblood B, Noto A, Porichis F, et al. Cutting edge: Prolonged exposure to HIV reinforces a poised epigenetic program for PD-1 expression in virus-specific CD8T cells. J Immunol **2013**; 191:540–4.
17. Bruniquel D, Schwartz RH. Selective, stable demethylation of the interleukin-2 gene enhances transcription by an active process. Nat Immunol **2003**; 4:235–40.
18. Murayama A, Sakura K, Nakama M, et al. A specific CpG site demethylation in the human interleukin 2 gene promoter is an epigenetic memory. EMBO J **2006**; 25:1081–92.
19. Kersh EN, Fitzpatrick DR, Murali-Krishna K, et al. Rapid demethylation of the IFN-gamma gene occurs in memory but not naive CD8T cells. J Immunol **2006**; 176:4083–93.
20. Ledderose C, Heyn J, Limbeck E, Kreth S. Selection of reliable reference genes for quantitative real-time PCR in human T cells and neutrophils. BMC Res Notes **2011**; 4:427.
21. Ishida T, Hamano A, Koiwa T, Watanabe T. 5' long terminal repeat (LTR)-selective methylation of latently infected HIV-1 provirus that is demethylated by reactivation signals. Retrovirology **2006**; 3:69.
22. Storey JD, Tibshirani R. Statistical significance for genomewide studies. Proc Natl Acad Sci U S A **2003**; 100:9440–5.
23. Holliday R, Pugh JE. DNA modification mechanisms and gene activity during development. Science **1975**; 187:226–32.
24. Jones PA, Liang G. Rethinking how DNA methylation patterns are maintained. Nat Rev Genet **2009**; 10:805–11.
25. Klose RJ, Bird AP. Genomic DNA methylation: the mark and its mediators. Trends Biochem Sci **2006**; 31:89–97.
26. Bird AP. CpG-rich islands and the function of DNA methylation. Nature **1986**; 321:209–13.
27. Gowers IR, Walters K, Kiss-Toth E, Read RC, Duff GW, Wilson AG. Age-related loss of CpG methylation in the tumour necrosis factor promoter. Cytokine **2011**; 56:792–7.
28. Lovinsky-Desir S, Ridder R, Torrone D, et al. DNA methylation of the allergy regulatory gene interferon gamma varies by age, sex, and tissue type in asthmatics. Clin Epigenetics **2014**; 6:9.
29. Thomas RM, Saouaf SJ, Wells AD. Superantigen-induced CD4+ T cell tolerance is associated with DNA methylation and histone hypo-acetylation at cytokine gene loci. Genes Immun **2007**; 8:613–8.
30. Thomas RM, Gao L, Wells AD. Signals from CD28 induce stable epigenetic modification of the IL-2 promoter. J Immunol **2005**; 174:4639–46.
31. Appay V, van Lier RA, Sallusto F, Roederer M. Phenotype and function of human T lymphocyte subsets: consensus and issues. Cytometry A **2008**; 73:975–83.
32. Romero P, Zippelius A, Kurth I, et al. Four functionally distinct populations of human effector-memory CD8+ T lymphocytes. J Immunol **2007**; 178:4112–9.
33. De Rosa SC, Brenchley JM, Roederer M. Beyond six colors: a new era in flow cytometry. Nat Med **2003**; 9:112–7.
34. Focosi D, Bestagno M, Burrone O, Petrini M. CD57+ T lymphocytes and functional immune deficiency. J Leukoc Biol **2010**; 87:107–16.
35. Palmer BE, Blyveis N, Fontenot AP, Wilson CC. Functional and phenotypic characterization of CD57+CD4+ T cells and their association with HIV-1-induced T cell dysfunction. J Immunol **2005**; 175:8415–23.
36. Kern F, Ode-Hakim S, Vogt K, Hoflich C, Reinke P, Volk HD. The enigma of CD57+CD28- T cell expansion–anergy or activation? Clin Exp Immunol **1996**; 104:180–4.
37. Monteiro J, Batliwalla F, Ostrer H, Gregersen PK. Shortened telomeres in clonally expanded CD28-CD8+ T cells imply a replicative history that is distinct from their CD28+CD8+ counterparts. J Immunol **1996**; 156:3587–90.
38. Strioga M, Pasukoniene V, Characiejus D. CD8+ CD28- and CD8+ CD57+ T cells and their role in health and disease. Immunology **2011**; 134:17–32.
39. Harari A, Vallelian F, Pantaleo G. Phenotypic heterogeneity of antigen-specific CD4T cells under different conditions of antigen persistence and antigen load. Eur J Immunol **2004**; 34:3525–33.